ADVANCED ENERGY & SUSTAINABILITY RESEARCH
Open Access
www.advenergysustres.com

Semiconductor Wafer Bonding for Solar Cell Applications: A Review

Katsuaki Tanabe

Wafer bonding is a highly effective technique for integrating dissimilar semiconductor materials while suppressing the generation of crystalline defects that commonly occur during heteroepitaxial growth. This method is successfully applied to produce efficient solar cells, making it an important area of research for photovoltaic devices. In this article, a comprehensive review of semiconductor wafer-bonding technologies is provided, focusing on their applications in solar cells. Beginning with an explanation of the thermodynamics of wafer bonding relative to heteroepitaxy, the functionalities and advantages of semiconductor wafer bonding are discussed. An overview of the history and recent developments in high-efficiency multijunction solar cells using wafer bonding is also provided. Bonded solar cells made of various semiconductor materials are reviewed and various types of wafer-bonding methods, including direct bonding and interlayer-mediated bonding, are described. Additionally, other technologies that utilize wafer bonding, such as flexible cells, thin-film transfer, and wafer reuse techniques, are covered.

1. Introduction

1.1. Photovoltaic Solar Cells

Global electricity consumption currently stands at around 3 terawatt (TW), while the world's total energy consumption is roughly 20 TW. Despite this high demand, the Earth receives an astonishing amount of solar energy. In fact, the solar constant—the amount of solar energy that reaches the top of the Earth's atmosphere—is estimated to be around 1.36 $kW \cdot m^{-2}$.[1,2] Given the Earth's cross-sectional area of $1.3 \times 10^8\,km^2$, this translates to a total solar power of 1.7×10^5 TW. In other words, the Earth receives as much solar energy in 1 h as the entire world uses in 1 year (or 10 min for electricity consumption). However, this energy is spread out over a vast area, so harvesting it efficiently requires covering a large surface with energy converters. This is where solar cells, also known as photovoltaics, come in. Photovoltaic devices, first discovered by the French scientist Henri Becquerel in 1839, convert sunlight directly into electricity by generating electron–hole pairs in a photovoltaic material. These pairs create a flow of current that follows the built-in potential slope of the material. Solar cells have emerged as an important alternative power source, especially since the oil crises in the 1970s. Additionally, solar cells are a promising carbon-free energy source that could help mitigate global warming. Achieving high efficiency solar energy conversion is crucial to making solar power a viable option for meeting the world's energy needs. The energy conversion efficiency of a solar cell refers to the ratio of the electric power generated by the cell to the amount of incident sunlight energy the cell receives per unit time.

1.2. Semiconductor Heterostructures

In a solar cell, one of the main causes of energy loss is the mismatch between the energy of incoming photons and the bandgap energy of the photovoltaic material. When the energy of a photon is lower than the bandgap energy, the solar cell cannot absorb it. In contrast, if the photon energy is higher than the bandgap energy, only the portion equal to the bandgap energy can be converted into electricity, with the excess energy being dissipated as heat. To mitigate this problem and increase the energy conversion efficiency, a type of structure called multijunction is commonly employed, where multiple photovoltaic materials with different bandgap energies are stacked together to form a tandem cell. This approach allows for more efficient absorption of a wider range of photon energies from the sunlight spectrum. Multijunction solar cells have been fabricated using a variety of materials including III–V compound semiconductors,[3–9] thin-film Si,[10–14] III–V/Si tandems,[15,16] organic semiconductors,[17–20] perovskite materials,[21,22] and perovskite/Si tandems.[23–26] Heterostructures or multilayer stacking of dissimilar semiconductor materials also play a crucial role in the wide range of optoelectronics field. They allow for the creation of band alignments that are not possible with a single material, leading to improved efficiency and performance. With the capability to engineer and manipulate the electronic and optical properties of semiconductor heterostructures, more efficient, compact, and versatile

K. Tanabe
Department of Chemical Engineering
Kyoto University
Nishikyo, Kyoto 615-8510, Japan
E-mail: tanabe@cheme.kyoto-u.ac.jp

The ORCID identification number(s) for the author(s) of this article can be found under https://doi.org/10.1002/aesr.202300073.

DOI: 10.1002/aesr.202300073

devices can be developed for various applications, including telecommunications, sensing, and energy harvesting.

1.3. Heteroepitaxial Growth and Crystalline Defects

Heteroepitaxial crystal growth is the most conventionally and widely used method to provide semiconductor heterostructures. This growth method involves depositing a crystalline film onto a substrate with a different lattice constant and crystal structure, which causes strain in the film due to lattice mismatch. The resulting strain leads to the formation of high-density dislocations in the crystal structure of the film, which can significantly impact its electrical properties. Specifically, dislocations can act as recombination centers for photoexcited electrical carriers, resulting in a loss of electric power in applications such as solar cells. Highly lattice-mismatched heterostructures will thus inevitably suffer from a large density of crystalline dislocations,[27–37] which severely degrade device performance. Therefore, it is important to develop strategies to minimize dislocation density to improve the quality and performance of heterostructured devices.

2. Semiconductor Wafer-Bonding Technology

2.1. What Is Semiconductor Wafer Bonding?

Wafer bonding is a fabrication process technique to integrate dissimilar semiconductor materials.[38–43] Two semiconductor wafers with flat surfaces are brought into contact with each other and then typically subjected to pressure and heat, which causes chemical bonds to form at the interface connecting the two materials. The wafer-bonding method is typically operated at significantly lower temperatures than the growth temperatures and can sustain the nonequilibrium state in the materials system, suppressing the generation of dislocations that would occur by strain relaxation during the transition into equilibrium. Therefore, the bonding method enables the production of high-performance heterostructured devices with low defect densities. While, the use of wafer bonding for device fabrication has some drawbacks, mainly attributed to the additional costs and machine time required for operating the bonding facility. Therefore, wafer bonding finds particular relevance in cases where superior device performance is highly demanded. As discussed in Section 4.2, there is a pressing need to explore and develop practical, cost-effective, and high-throughput wafer-bonding techniques. Wafer bonding has been employed to fabricate a variety of electronic and photonic devices, including field-effect transistors,[44–46] light-emitting diodes,[47–51] semiconductor lasers,[52–59] optical modulators,[60–62] photodetectors,[63–65] solar cells, and advanced concepts in optoelectronics.[66–74] Textbooks[75–78] and review articles[79–88] on wafer-bonding technologies and applications are available. Semiconductor wafer bonding is a crucial process used in various industries to integrate different materials and create complex structures. Several industrial technologies for wafer bonding exist, each with its specific applications and advantages. While various bonding techniques tailored for solar cell applications will be discussed in Section 4.2–4.5, let us briefly review here some prevalent industrial wafer-bonding methods utilized in a broader range of semiconductor fields. Direct wafer bonding, also known as molecular bonding or fusion bonding, involves bringing two semiconductor wafers into close contact under controlled conditions, typically at elevated temperatures and in a clean environment. The bond formation occurs at the atomic or molecular level, resulting in a strong and permanent bond without the need for adhesives. This technique is used to integrate different materials, such as silicon-on-insulator wafers or for wafer stacking to create 3D structures. Eutectic bonding is employed for materials with a eutectic point, which refers to a specific temperature at which the solid components of an alloy melt to form a low-temperature liquid phase. When two wafers with complementary eutectic materials are brought together at the eutectic temperature, the materials melt and form a strong bond. This technology is often used in applications requiring excellent thermal conductivity, such as infrared sensors. Anodic bonding is a method that utilizes an electrostatic field and elevated temperature to bond a glass or silicon wafer to another silicon wafer. The glass wafer contains alkali ions that migrate toward the silicon wafer under the influence of the electric field, creating a strong bond between the two materials. Anodic bonding is commonly used for applications requiring hermetic sealing, such as microelectromechanical systems (MEMS) devices and certain sensors. Adhesive wafer bonding involves the use of intermediate adhesives or bonding agents to join two wafers together. The adhesive can be a polymer, epoxy, or other material that is applied as a thin layer between the wafers. Adhesive bonding allows for more flexibility in material selection and is often used in heterogeneous integration processes. Wafer bonding with solid intermediate layers is also widely used. In this method, an intermediate layer is introduced between the wafers to facilitate bonding. This intermediate layer can be an oxide, nitride, or other thin-film material that promotes adhesion between the wafers. This approach allows for precise control over the bonding process and can be used for various applications, including MEMS and power devices. These are some of the commonly used industrial technologies for semiconductor wafer bonding. Each technique has its strengths and limitations, making them suitable for different applications across the electronics and optics industries. While current research laboratory studies mainly focus on experiments using relatively small semiconductor wafers or diced pieces, there have been a number of reports of bonding of full 4-, 6-, and 8-inch wafers.[89–92] The wafer-bonding scheme may be easily extended to larger wafers.

2.2. Thermodynamics of Semiconductor Wafer Bonding

The strain relaxation process in wafer-bonded semiconductor heterostructures was numerically investigated, relative to those formed by epitaxial growth.[93] The calculations revealed a slow strain relaxation behavior in lattice-mismatched heterostructures wafer bonded at lower temperatures than those used in epitaxial growth. By sustaining the material system at a metastable state, the thermodynamically preferred dislocation generation is suppressed. **Figure 1** summarizes the time-constant values for wafer bonding, extracted from the time-evolving strain relaxation data in numerical simulations for each wafer-bonding temperature,

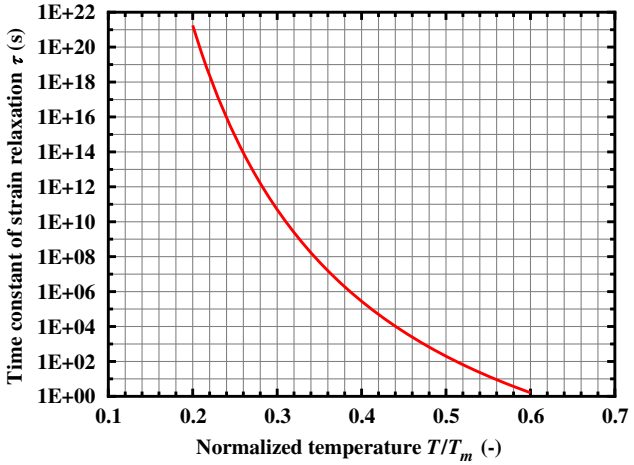

Figure 1. Dependence of the time constant of strain relaxation, τ, on the normalized temperature, T/T_m, for a lattice mismatch of 0.04 for wafer bonding. Reproduced with permission.[93] Copyright 2021, Institute of Physics.

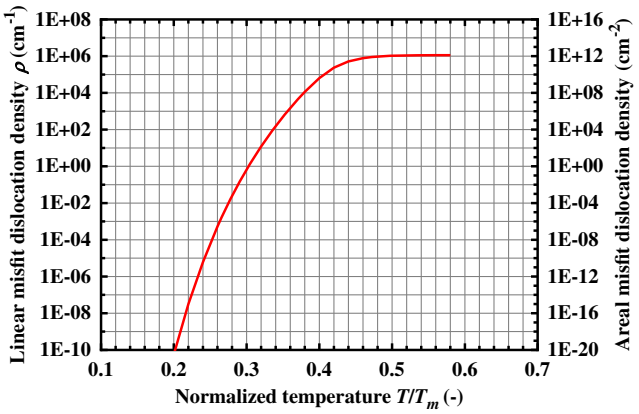

Figure 2. Dependence of the linear density of misfit dislocations, ρ, on the normalized temperature, T/T_m, for a lattice mismatch of 0.04 for 1 h wafer bonding. Adapted with permission.[93] Copyright 2021, Institute of Physics.

normalized by the melting temperature of the semiconductor material, T/T_m. The lattice mismatch between the two crystalline materials was set to 0.04, accounting for the lattice mismatch in the heterointerfaces of common bonded material combinations, such as GaAs/Si, InP/GaAs, and Ge/Si. Note that the thermal stress could also be a cause of dislocation generation, but the thermal expansion coefficient mismatch in these heterostructures is about 0.001 or less,[94–96] and therefore its contribution is negligible relative to that of the lattice mismatch. The typical range of T/T_m for wafer bonding is 0.2–0.4. For T/T_m of 0.4 and 0.3, the time constant of strain relaxation, τ, was observed to be approximately as 3×10^5 s (80 h) and 5×10^{10} s (1600 years), respectively. T/T_m of 0.2 roughly corresponds to room-temperature wafer bonding, or devices under operation or at rest. At this normalized temperature, τ was 2×10^{21} s, which corresponds to 6×10^{13} years. In contrast, τ was independently calculated to be as small as 14 s for the case of heteroepitaxial growth at a typical normalized temperature, T/T_m, of 0.6. To explicitly quantify the misfit dislocation density generated in the wafer-bonding process, **Figure 2** plots the calculated linear density of misfit dislocations, ρ, at the point of 1 h, as a typical duration of the thermal process in wafer bonding, in the numerical simulation for each temperature condition, T/T_m. For example, Figure 2 shows that ρ is 10 cm^{-1} (or an areal density of 1×10^2 cm^{-2}) for T/T_m of 0.32. This misfit dislocation density implies only one dislocation per millimeter, which is insignificant and causes minimal disturbance to the semiconductor crystals during wafer bonding. In contrast, a higher T/T_m of 0.38 leads to ρ of 1×10^4 cm^{-1} (1×10^8 cm^{-2}), corresponding to a dislocation pitch of 1 µm. Such low densities of misfit dislocations achieved through wafer bonding make it a technically advantageous approach for fabricating semiconductor heterostructures. The low operating temperature of wafer bonding allows for slow strain relaxation, which suppresses thermodynamically preferred dislocation generation, leaving the lattice-mismatched heterostructure at a nonequilibrium, metastable state. The difference in operating temperatures can be attributed to the fact that wafer bonding connects a pair of preformed crystalline materials, whereas epitaxial growth requires high temperatures for the diffusion of surface adatoms during deposition. In contrast, for heteroepitaxy at T/T_m of 0.6, it was independently calculated that even a 1 min growth generates a large ρ of 1×10^6 cm^{-1} (1×10^{12} cm^{-2}). Thus, the nonequilibrium crystalline stability in the wafer-bonded semiconductor heterostructures was evidenced. This calculation emphasizes the nonequilibrium crystalline stability in wafer-bonded semiconductor heterostructures. Owing to such a mechanism, semiconductor wafer bonding is promising to generate lattice-mismatched semiconductor heterostructures with low defect densities, which are otherwise difficult to obtain by the conventional epitaxial growth method.

3. Wafer Bonding for Various Photovoltaic Materials

3.1. Bonded all-III–V Multijunction Solar Cells

3.1.1. Subcell Interconnection by Wafer Bonding

Currently, wafer-bonded solar cells are mainly used in multijunction cells made entirely of III–V semiconductor compounds. This is partly due to the superior energy conversion efficiencies achieved by III–V materials compared to other types of solar cells, such as Si, CdTe, CuInGaSe (CIGS), dye-sensitized, organic, and perovskite. The all-III–V tandem approach demands greater flexibility in constructing heterostructures to achieve even higher efficiencies. Before the emergence of wafer bonding in the photovoltaic community, the heteroepitaxially grown InGaP/GaAs dual-junction and InGaP/(In)GaAs/Ge triple-junction systems had the prosperity of highest efficiencies consistently from about 30% around 1995 to about 40% around 2010.[3–8] The $In_{0.5}Ga_{0.5}P$, GaAs, and Ge crystals are almost lattice-matched to one another, and therefore ideal for epitaxial growth in terms of the suppression of dislocation generation. Their bandgap energies ($In_{0.5}Ga_{0.5}P$: 1.9 eV, GaAs: 1.4 eV, and Ge: 0.67 eV) were also well suited for covering the solar

spectrum. However, using Ge as the material for the bottom subcell in a triple-junction solar cell is not optimal because the InGaP/GaAs/Ge cell is not current-matched. The Ge subcell generates about twice as much photocurrent as the other subcells, resulting in half of the photocurrent being wasted in the series connection of subcells. Fabricating a multijunction solar cell with an ideal combination of semiconductor-material bandgap energies by the growth method was thus challenging due to the lattice-matching restriction. To improve the efficiency, it would be preferable to replace the Ge subcell with an alternative semiconductor with a bandgap energy around 1.0 eV or insert such a semiconductor between the GaAs and Ge subcells.

In this context, by integrating InP-based semiconductors with the GaAs (Ge)-based subcell system, we could significantly enhance the flexibility of material choices, to approach the multijunction structure with the ideal combination of bandgap energies. Nevertheless, the lattice mismatch of 4% between GaAs (Ge) and InP crystals severely hinders heteroepitaxial growth with low dislocation densities, as discussed in the previous section. As a prototype for GaAs-based/InP-based combination heterostructures, in 2006, a monolithic GaAs/$In_{0.5}Ga_{0.5}As$ dual-junction solar cell was fabricated by direct wafer bonding.[97] In this study, an Ohmic-characteristic GaAs/InP-bonded heterointerface was realized. The $In_{0.5}Ga_{0.5}As$ lower subcell material was lattice-matched to InP. The GaAs and $In_{0.5}Ga_{0.5}As$ photovoltaic layers were epitaxially grown on GaAs and InP substrates, respectively. Then, the upper GaAs subcell and the lower $In_{0.5}Ga_{0.5}As$ subcell with an InP window layer atop were bonded to each other, followed by the removal of the GaAs substrate by chemical etching. **Figure 3** illustrates a fundamental wafer-bonded multijunction solar cell structure in contrast to a heteroepitaxially grown cell. Open-circuit voltage and quantum efficiency measurements for the bonded GaAs/InGaAs dual-junction cell and reference individual unbonded GaAs and InGaAs single-junction subcells verified that the wafer-bonding process did not degrade the crystalline quality of each semiconductor material. This study indicated the potential for a InGaP/GaAs/InGaAsP/InGaAs four-junction solar cell by bonding a GaAs-based lattice-matched InGaP/GaAs dual-junction subcell to an InP-based lattice-matched InGaAsP/InGaAs dual-junction subcell.[97] In 2014, a four-junction solar cell using the wafer-bonding scheme renewed the highest efficiency among all types of solar cells, reaching 44.7%.[98] The record-efficiency cell was composed of 1.9 eV $In_{0.5}Ga_{0.5}P$, 1.4 eV GaAs, 1.1 eV $In_{0.8}Ga_{0.2}As_{0.3}P_{0.7}$, and 0.74 eV $In_{0.5}Ga_{0.5}As$ (**Figure 4**). The upper InGaP/GaAs dual-junction subcell and the lower InGaAsP/InGaAs dual-junction subcell were epitaxially grown on GaAs and InP substrates, respectively, and bonded to each other. The advantage in the device performance of the wafer-bonding scheme over heteroepitaxy was thus demonstrated. Importantly, the current world record for solar cell efficiency, 47.6%, has also been achieved by a similar four-junction structure fabricated using wafer bonding.[99,100] Moreover, other types of III–V multijunction solar cells fabricated by wafer bonding have reported energy conversion efficiencies exceeding 40%.[101–103] Although the energy conversion efficiency values of solar cells discussed in this review are mainly the highest achieved under concentrated illumination, typically ranging in several tens to thousands of suns, a wafer-bonded 2.2/1.7/1.4/1.1/0.73 eV five-junction cell has achieved the current record efficiency of 38.8% under 1 sun, AM1.5G spectrum for a large-area cell ($>1\ cm^2$).[100,101]

3.1.2. Inverted Growth and Bonding Scheme

The previous section noted that Ge is not the optimal choice as the bottom subcell in triple-junction solar cells. Instead, researchers have used an alternative approach involving the growth of a 1.0 eV $In_{0.3}Ga_{0.7}As$ subcell, lattice-mismatched to GaAs by 2%, on an inversely grown GaAs/InGaP dual-junction subcell via compositionally graded layers.[104,105] Au was electroplated on the top surface of the grown structure, as the bottom electrode in the inverted device. The electroplated surface of the structure was then bonded to a supporting Si wafer via epoxy glue, followed by the removal of the GaAs substrate by chemical etching,

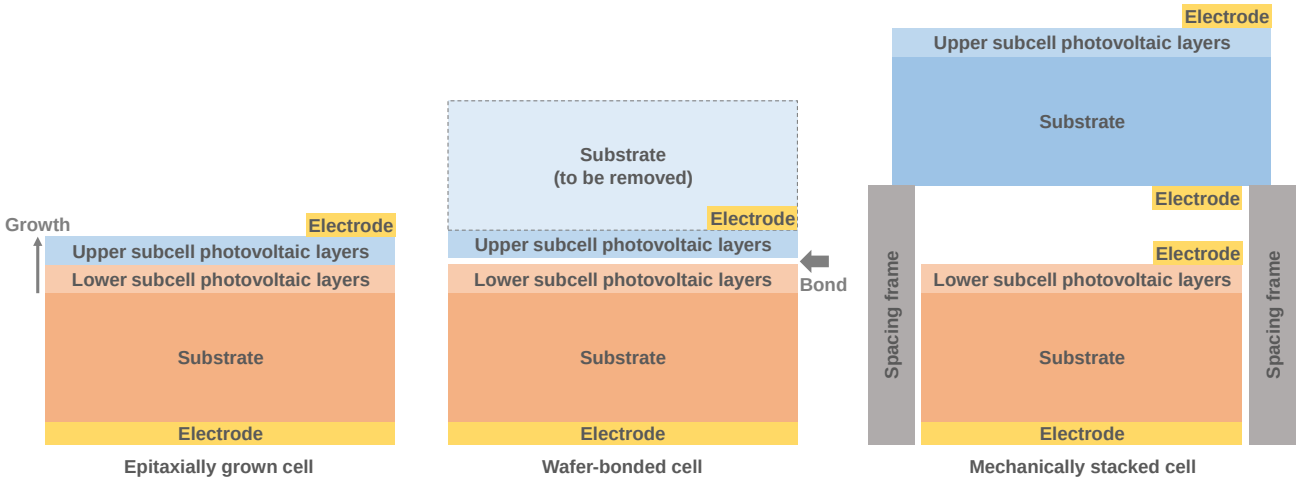

Figure 3. Fundamental cross-sectional schematics of typical multijunction solar cells fabricated by (left) heteroepitaxial growth, (middle) wafer bonding, and (right) mechanical stacking. The photovoltaic layers comprise, e.g., an n^+-type window, an n-type emitter, a p-type base, and a p^+-type back surface field in the order from top to bottom.

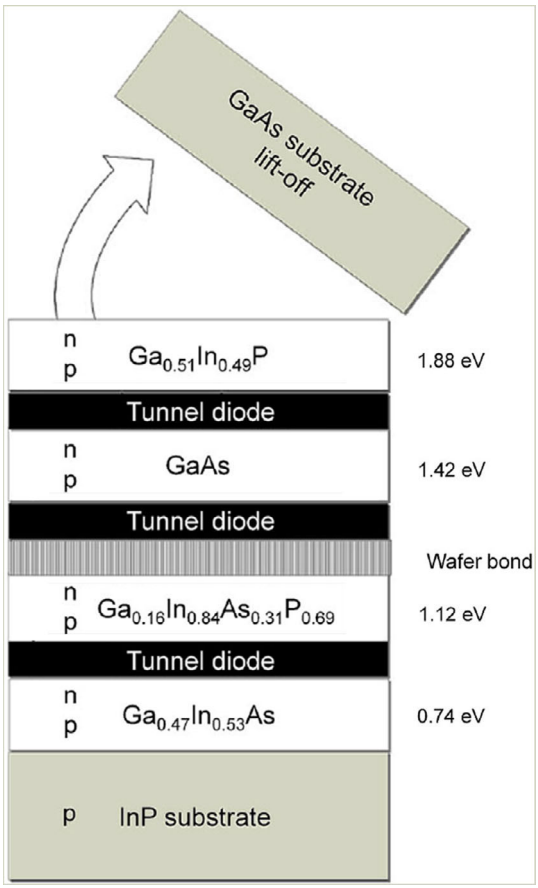

Figure 4. Schematic cross-sectional diagram of the four-junction wafer-bonded solar cell, indicating the composition of the subcell materials with bandgap energies, the location of tunnel diodes, and the wafer bond. Reproduced with permission.[98] Copyright 2014, Wiley-VCH.

resulting in an InGaP/GaAs/InGaAs triple-junction cell. This approach set a record efficiency of 40.8% in 2008.[106] Furthermore, a six-junction cell comprising 2.1 eV $Al_{0.2}In_{0.5}Ga_{0.3}$ P, 1.7 eV $Al_{0.2}Ga_{0.8}As$, 1.4 eV GaAs, 1.2 eV $In_{0.2}Ga_{0.8}As$, 0.95 eV $In_{0.3}Ga_{0.7}As$, and 0.69 eV $In_{0.6}Ga_{0.4}As$ established another record efficiency of 47.1% in 2019, by using a similar scheme of inverted metamorphic growth (**Figure 5**).[107,108]

3.2. Bonded III–V/Si Multijunction Solar Cells

While all-III–V multijunction solar cells were discussed earlier, devices composed entirely of III–V semiconductors are associated with high production costs. In contrast, Si has several advantages, including its low cost, lightweight, environmental friendliness, high mechanical and thermal stability, and high thermal conductivity. By integrating III–V compound semiconductor photovoltaic thin films onto Si substrates, we can therefore potentially improve device performance and reduce manufacturing costs. In addition, according to our calculations using the detailed balance limit scheme,[109,110] a 1.7 eV/1.1 eV (Si) bandgap two-terminal dual-junction solar cell has a theoretical efficiency upper limit of 48% under 1000 suns, AM1.5D spectrum (or 41% under 1 sun, AM1.5G), which is comparable to the experimental efficiencies of state-of-the-art all-III–V four–six junction cells.[98–103,107,108] It's worth noting that the current record-efficiency cell (35.5%) among dual-junction cells, consisting of 1.7 eV $In_{0.3}Ga_{0.7}As_{0.3}P_{0.7}$ and 1.1 eV $In_{0.2}Ga_{0.8}As$,[100,111] also indicates the promise of the 1.7 eV/1.1 eV combination. Therefore, utilizing Si-based dual-junction structures rather than all-III–V tandems can result in solar cells with lower cost, lighter weight, and even higher efficiency by minimizing inter-subcell losses. As an approach for this ideal bandgap combination, 1.7/1.1 eV $Al_{0.2}Ga_{0.8}As$/Si dual-junction solar cell was fabricated by using GaAs/Si direct wafer bonding, overcoming a 4% lattice mismatch (**Figure 6**).[112,113] This study indicated that such a

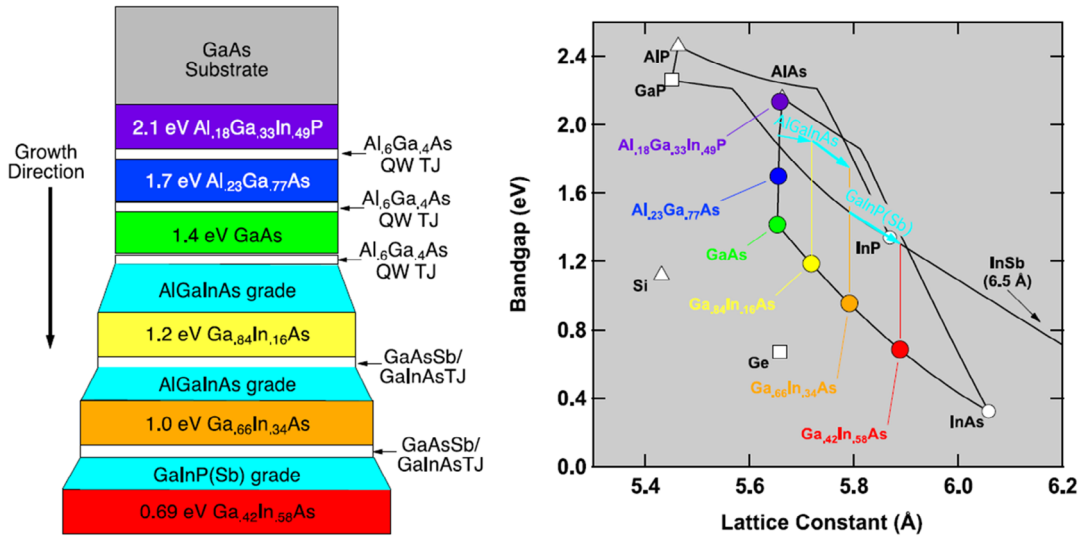

Figure 5. Six-junction inverted metamorphic solar cell: (left) schematic cross-sectional diagram and (right) bandgap energies of the subcell materials in dependence on lattice constant. Reproduced with permission.[107] Copyright 2018, American Institute of Physics.

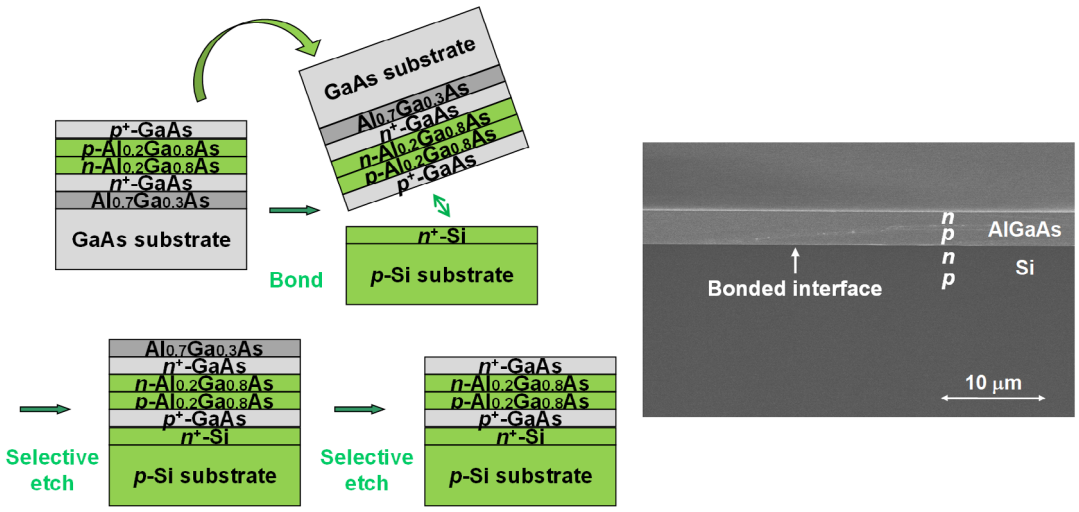

Figure 6. AlGaAs/Si dual-junction solar cell: (left) schematic flow diagram of the fabrication process and (right) cross-sectional scanning microscope image.[112,113]

wafer-bonding interconnection approach is extendable to other photovoltaic heterojunctions where lattice mismatch accommodation is a challenge, enabling the realization of next-generation ultrahigh efficiency multijunction solar cells such as a InGaN/AlGaAs/Si/Ge four-junction cell. In this context, a variety of wafer-bonded III–V-on-Si multijunction solar cells have been generated,[114–118] primarily GaAs-based III–V/Si tandems. Meanwhile, InP and its lattice-matched compounds are also a promising semiconductor material family owing to their high photovoltaic efficiencies[119–122] and radiation tolerance,[123,124] which are particularly advantageous for space applications. However, the InP/Si heterostructure has a considerable crystalline lattice mismatch of 8% between InP and Si, significantly larger than those of GaAs/InP (4%) and GaAs/Si (4%), which further hinders the conventional heteroepitaxial growth. Nevertheless, directly bonded Ohmic InP/Si heterostructures have been realized, overcoming such a large lattice mismatch, with a demonstration of InP solar cells bonded on Si substrates.[125,126] The InP/Si direct-bonding technology may also enable the realization of ultrahigh efficiency multijunction solar cells composed of InP and Si-based subcell sets, such as an AlAsSb/AlInAs/InP/Si/SiGe five-junction cell. The AlAsSb (1.9 eV) and AlInAs (1.5 eV) materials are lattice-matched to InP,[127–129] and the SiGe material (0.67–1.1 eV) can be grown on Si substrates with graded buffer layers.[130,131]

3.3. Bonded III–V/CIGS Multijunction Solar Cells

CuInGaSe (CIGS), a I–III–VI_2 compound semiconductor, has advantages as a photovoltaic material, including its low cost, high efficiency,[132–134] and excellent radiation tolerance.[135,136] Particularly for the purpose of space use, InGaP/GaAs/CIGS triple-junction solar cells were fabricated by using metal-particle-mediated wafer bonding.[137,138] Testing of the bonded III–V/CIGS multijunction cells confirmed their superior radiation resistance compared to the typical InGaP/GaAs/InGaAs triple-junction space solar cells.

3.4. Bonded Organic Solar Cells

Organic solar cells are a promising solution for their cost-effectiveness and lightweight properties.[139–142] Commonly, organic photovoltaic devices are fabricated through sequential layer-by-layer deposition or coating of the donor and acceptor organic semiconductors. As an alternative fabrication technique, a donor and acceptor organic polymer materials were individually deposited onto conductive glass substrates, and then the donor and acceptor layers were bonded to each other.[143–146] This fabrication scheme ensures that the donor material has proper contact with the higher-work-function contact and the acceptor with the lower-work-function contact. In addition, such a method can minimize molecular disordering or intermixing to preserve the structure of each surface, for the convenience of the characteristics tuning and analysis, in contrast to the conventional wet process. This bonding approach further eases the modification of each of the donor and acceptor surfaces, resulting in an interlayer to control carrier transport properties.

4. Various Wafer-Bonding Methods for Solar Cell Applications

4.1. Mechanical Stacking

Prior to the development of wafer bonding, simple stacking of two cells on top of each other with a spacing frame, so-called mechanical stacking, was used to fabricate four-terminal multijunction solar cells, as a simple strategy to circumvent the lattice-mismatching problem in heteroepitaxial growth (Figure 3).[147–150] This technique offers advantages such as freedom from current-matching conditions and electrical resistance at the tunneling junction in heteroepitaxy or the bonded heterointerface. In contrast, this approach suffers from drawbacks such as optical loss due to the refractive-index mismatch between the semiconductors and the air gap, as well as difficulties in using

the electrical output from independent subcells. Nonetheless, in four-terminal configurations, high total energy conversion efficiencies were achieved, including 31.1%, 32.6%, and 33.3% for mechanically stacked GaAs/InGaAsP,[150] GaAs/GaSb,[147] and InGaP/GaAs/InGaAs[148] dual- and triple-junction cells, respectively.

4.2. Direct Semiconductor Wafer Bonding

Semiconductor-to-semiconductor direct wafer bonding without a mediating material is the most standard method for solar cell applications. In contrast, bonding technologies such as welding or adhesive-mediated bonding have been commonly used in the wider field of bonding, such as in the bonding of metals. While a thick[55,82] or thin[52,53,63] oxide layer is often employed as a mediating interlayer in wafer bonding for optoelectronics, it is rarely used for solar cell applications due to the electrically insulating characteristics of oxides. For solar cell applications, electrical conductivity and optical transparency are required in the bonded interfaces. Because of these basic demands, semiconductor-to-semiconductor direct bonding has been considered most suitable for photovoltaic applications, and most commonly employed. Nevertheless, direct wafer bonding is generally more difficult than bonding methods with mediating agents, as direct bonding is highly sensitivity to surface roughness and particulates. A photovoltaic structure comprising semiconductor layers formed by epitaxial growth typically has some surface roughness, which can make it difficult to establish a firm contact in direct bonding with solid semiconductor surfaces with a root-mean-square roughness above a couple of nanometers.[113] Moreover, direct bonding is more affected by environmental conditions represented by airborne particles, compared to other bonding schemes mediated by soft, deformable adhesive agents. Particle contamination can reduce the interfacial stability and conductivity in wafer bonding, which is why the process is typically carried out in cleanrooms with low particle densities of around 1000 m^{-3}, leading to high operation costs. While most processes related to electrical and optical devices are performed in cleanrooms, some categories of large-area, relatively impurity-insensitive devices, such as solar cells, could be fabricated in a normal atmosphere. The commercialization of photovoltaic solar panels is highly sensitive to the areal production cost of the cells, and avoiding the use of cleanrooms would be a priority. In this context, direct wafer bonding in a non-cleanroom, regular ambient with a particle density of 5×10^6 m^{-3} along with a cell fabrication demonstration has recently been reported, by implementing proper surface pretreatments based on the correlations among surface treatments, particle densities, bonding strengths, and interfacial conductivities.[151] Although the wafer-bonded solar cell field is currently in the fundamental, lab-scale research stage, the potential issue of cell production cost may become a critical factor in future commercialization. Therefore, developing cost-effective process schemes that eliminate the need for cleanrooms can be crucial for the successful commercialization of photovoltaic solar panels.

4.3. Metal-Mediated Wafer Bonding

The metal-mediated wafer-bonding technique is also widely used for optoelectronic device applications.[45,47,48,56,57,152–156] For III–nitride semiconductor devices such as GaN and InGaN light sources,[47,48,154,156] the growth substrates are typically electrically insulating or difficult to apply low-resistivity Ohmic metal contacts. Therefore, transferring the optically active III–nitride layers onto electrically conductive substrates after epitaxial growth is often necessary. Therein, the metal bonding interlayer can also act as an optical reflective mirror. Meanwhile, for multijunction solar cell applications, using a metal-bonding interlayer can cause substantial optical shadow loss for the subcells beneath the bonded interface, which would limit the overall multijunction cell current in series electrical connection. Still, the metal-mediated wafer-bonding method has several advantages, such as the allowance for higher electrical conductance, lower bonding temperature, and higher surface roughness tolerance. Instead of using a simple, uniform sheet of metal-bonding interlayer, wafer-bonding techniques mediated by metal nanoparticles have been developed.[157–160] For multijunction solar cell applications, bonding mediated by patterned or self-assembled micro-/nanoscale metal structures were employed.[161–166] By sufficiently reducing the areal density of metal nanoparticles or aligning the bonding metal structures right beneath the top metal electrode patterns, the optical shadow loss can be minimized. The optical reflection loss caused by the refractive index mismatch due to the existence of air gaps at the bonded interface for the locations in the absence of the metal structures could be an issue. However, employing metal structures sufficiently thinner than the wavelengths of the incident solar spectrum may minimize the reflection loss.

4.4. Wafer Bonding Mediated by Transparent Conductive Agents

The surface condition of the wafer is severely restricted in direct bonding and bonding mediated by solid-state materials like metals or oxides because surface roughness and particulates can negatively impact interfacial stability and conductivity. Optical transparency of the bonded interface is also a crucial factor in multijunction solar cell applications. For the purpose of acquiring higher electrical conductivity and surface roughness tolerance than the case of semiconductor-to-semiconductor direct wafer bonding, transparent conductive oxide (TCO) materials, such as indium tin oxide, zinc oxide, and indium zinc oxide, have been considered as bonding agents for photovoltaic applications.[167–171] Nevertheless, TCO-mediated bonding can cause optical loss due to the refractive-index contrast between the semiconductor and TCO. As a rough estimate, a single semiconductor/TCO interface would have a reflectivity of 16% for refractive indices of 3.5 and 1.5, respectively. Therefore, a TCO interlayer with a thickness sufficiently larger than the optical wavelength would result in a net reflectivity of 29%. However, for the interlayer thicknesses around the order of the optical wavelengths, the reflectivity varies in an oscillating manner on the interlayer thickness and the optical wavelength. Therefore, the reflectivity can be controlled by adjusting the TCO thickness, depending on the application. In addition, such an interfacial reflectance could be positively utilized for current matching in multijunction solar cells by tuning the TCO interlayer thickness. Moreover, the reflectance can be eliminated by employing a TCO

thickness sufficiently smaller than the optical wavelength, although this approach requires a trade-off with surface-roughness tolerance.

Other types of semiconductor wafer-bonding methods mediated by transparent conductive materials have been proposed and experimentally demonstrated for solar cell applications, including those that use hydrogels,[172] polymer–particle composites,[173] and carbon nanotube composites.[174] Such soft matter–based bonding techniques also have the potential to serve as temporary adhesives. For instance, hydrogels can provide adhesion and detachment that can be used to protect semiconductor wafer surfaces during storage or carriage,[175] as well as transfer and print semiconductor thin films onto different substrates.[56,71,144,145] **Table 1** summarizes the advantages and disadvantages of the various methods employed in the formation of semiconductor heterostructures.

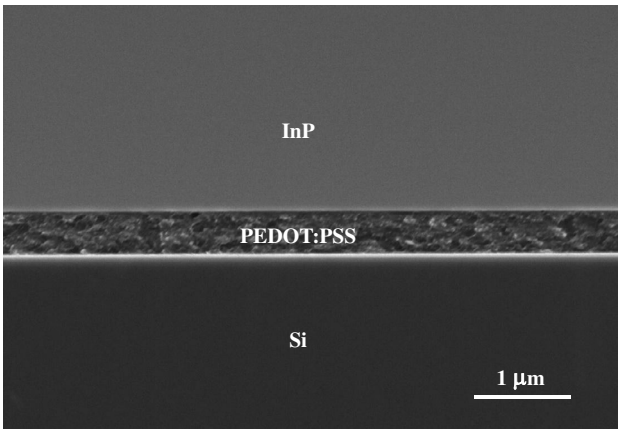

Figure 7. Cross-sectional scanning electron microscope image of the bonded InP/PEDOT:PSS/Si heterostructure. Reproduced with permission.[178] Copyright 2023, Institute of Physics.

4.5. Functional Bonding

Conventionally, interfacial bonding agents in semiconductor wafer bonding have served as a means of assisting mechanical adhesion and/or electrical conductance. The concept of functional bonding was recently proposed to achieve both bonding formation and optoelectronic function implementation simultaneously.[176–178] This scheme utilizes appropriate functional materials as the bonding agent, which can improve manufacturing efficiency.

4.5.1. Wafer Bonding Mediated by Photovoltaic Materials

First, a novel concept of semiconductor wafer bonding that simultaneously enables bond formation and solar cell implementation was proposed and experimentally demonstrated.[178] As an experimental example, utilizing the characteristics of poly(3,4-ethylenedioxythiophene) poly(styrenesulfonate) (PEDOT:PSS)/Si heterojunction solar cells,[179–181] PEDOT:PSS-mediated InP/Si wafer bonding was conducted. The resulting InP/PEDOT:PSS/Si heterostructure (**Figure 7**) demonstrated that the PEDOT:PSS/Si heterojunction formed at the bonded interface can operate as a photovoltaic device.[178] This bonded heterostructure serves as a prototype architecture for the photovoltaic functional bonding concept, representing an intermediate section of a multijunction solar cell with a built-in subcell. If the InP layer is considered as the upper subcell of a multijunction cell, the PEDOT:PSS/Si heterojunction solar cell part, which is formed during the bonding process, can be regarded as the lower subcell. This simple semiconductor bonding scheme, mediated by functional agents that generate built-in subcells, has the potential to enable low-cost, high-throughput production of high-efficiency multijunction solar cells.

4.5.2. Wafer Bonding Mediated by Wavelength-Conversion Materials

Second, the concept of wavelength conversion material–mediated semiconductor wafer bonding was proposed and demonstrated.[176,177] The most crucial obstacle for solar cell efficiency is the mismatch between the energy of incoming photons and the bandgap of photovoltaic materials, as discussed in the introductory section on multijunction solar cell mechanism. As an approach for addressing this challenge, one can convert a part of the solar spectrum into a more suitable spectral light for each photovoltaic material to absorb. The use of photonic up and down conversion for solar cell applications have been explored theoretically[182–186] and experimentally.[187–191] Employing wavelength-converting materials as the bonding agent allows for simultaneous bond formation and interfacial optical functionality generation. In preliminary studies, a hydrogel matrix embedded with rare-earth doped upconversion nanoparticles[177] and fluorescent downconversion particles[176] have been used to mediate semiconductor wafer bonding. The bonded interfaces exhibited both wavelength-converting functionality and electrical conductivity, demonstrating their applicability to photovoltaic devices. Enhanced photocurrent in bonded Si solar cells with

Table 1. Summary of the advantages and disadvantages of the various methods employed in the formation of semiconductor heterostructures.

	Heteroepitaxial growth	Mechanical stacking	Direct semiconductor wafer bonding	Metal-mediated wafer bonding	Wafer bonding mediated by transparent conductive agents
Lattice mismatch allowance	Low	High	High	High	High
Surface roughness tolerance	Low	High	Low	High	High
Interfacial electrical conductance	High	N/A	Moderate	High	Moderate
Interfacial optical conductance	High	Moderate	High	Low	Moderate
Additional process/cost	N/A	Very large	Large	Very large	Very large

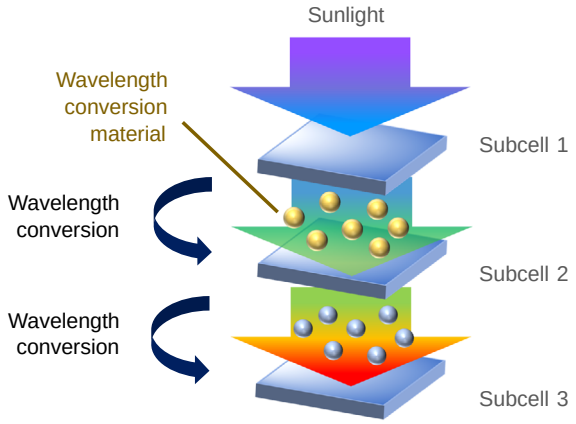

Figure 8. Conceptual illustration of the use of wavelength conversion material–mediated wafer bonding for multijunction solar cell applications.[176,177]

the upconversion material was observed.[177] This bonding and interfacial scheme could be useful in improving the performance and structural flexibility of multijunction solar cells by photon management and current matching among the subcells, by converting the wavelength of the light transmitted through the upper subcell to one that is highly absorbed by the lower subcell (**Figure 8**). For example, an upconverting interface in a multijunction solar cell could enable the use of inherently non-absorbed longer-wavelength light in the lower subcell, thus enhancing the overall energy conversion efficiency. In addition, this approach suggests the possibility of efficiently using excess or leftover Si solar cells; attaching an additional Si cell to an original Si cell via upconversion material–mediated bonding may be able to boost the electrical output.

5. Other Photovoltaic Applications of Wafer Bonding

5.1. Lightweight, Flexible Solar Cells on Plastic Films

Semiconductor substrates made of materials such as crystalline Si, Ge, GaAs, and InP for solar cells are typically expensive, heavy, thick, and solid. There is growing interest in developing photovoltaic modules with low-cost, lightweight, and mechanically flexible support substrates, which are suitable for a number of applications including portable electronic devices, wearable technology, and aerospace use.[192–201] There are three approaches for producing flexible solar cells: 1) using arrays of small-scale cells integrated on flexible films,[192,197,199] 2) growing amorphous photovoltaic materials such as amorphous Si, CIGS, and organic semiconductors directly on flexible films,[193,198,201] and 3) transferring crystalline photovoltaic materials from their original substrates onto flexible films.[194–196,200] Direct growth of photovoltaic semiconductor thin films on plastic films or metallic foils as substrates would be the most desirable approach, taking into account the loss of intercell spacings and fabrication simplicity. However, crystalline semiconductor materials cannot be grown on noncrystalline substrates, leading to poor performance of amorphous cells. To overcome this limitation, a method of preparing crystalline cells on noncrystalline substrates is by transferring photovoltaic semiconductor layers grown in advance on proper crystalline substrates onto noncrystalline substrates using a bonding technique. For example, crystalline photovoltaic layers were grown on a lattice-matched crystalline substrate, and the top surface was then bonded upside down to a plastic film.[194,196,200] The original growth substrate was removed by chemical etching, leaving a flexible solar cell device consisting of thin-film photovoltaic layers sitting on a plastic film (**Figure 9**).

5.2. Thin-Film Solar Cells with Metallic Bottom Structures

Wafer bonding offers significant design flexibility for solar cell structures. For example, the bonding technique allows the fabrication of solar cells with photovoltaic layers of arbitrary thickness sitting on arbitrary substrates. This is in contrast to conventional epitaxially grown solar cell structures, where the photovoltaic layer must be directly connected to a thick crystalline substrate lattice-matched to the photovoltaic layer. Thinner photovoltaic layers absorb less light, while thicker layers suffer from more bulk carrier recombination, both of which reduce the cell's electrical output. To optimize efficiency, the thickness of the active photovoltaic layer must balance these competing factors. Direct-bandgap semiconductors such as GaAs and InP have significantly shorter absorption lengths than their wafer thickness. As a result, they suffer from bulk carrier recombination loss in the thick substrates, leading to a reduction in the cell's output current and voltage. Therefore, it is desirable to remove the thick growth substrate or replace it with a metal plate acting as an electrode and optical mirror that reflects the unabsorbed sunlight component in the first path. To address this structural demand, an ultrathin GaAs cell structure with a metallic back layer was proposed and experimentally demonstrated using wafer bonding and layer transfer techniques.[202] This cell consisted of a 30 nm thick p-InGaP window, 50 nm p-GaAs emitter, 50 nm n-GaAs base, and 30 nm n-InGaP back surface field (i.e., 160 nm thick in total) on a metal layer on a Si substrate (**Figure 10**). This ultrathin, backside-metallized GaAs cell showed significant enhancements in short-circuit current density and efficiency relative to the reference GaAs cell with an absorbing GaAs back layer due to a Fabry–Pérot resonance in the air/semiconductor/metal heterostructure.[202] Improvements in cell performance through the use of thin photovoltaic layers on metallic structures have subsequently been reported.[203,204] The current record efficiency for single-junction solar cells, 29.1%, was achieved by a thin-film GaAs cell layer transferred onto a metallized flexible film.[100,205]

5.3. Wafer Reuse Technologies

To enable widespread use of photovoltaic modules as a primary source of alternative electricity, it is essential to reduce the production cost of solar cells. One promising approach is the reuse of expensive crystalline semiconductor substrates from high-efficiency cells. The most well-known scheme of wafer reuse for III–V compound semiconductor cells is the epitaxial liftoff of GaAs-based thin films by utilizing selective wet chemical etching of AlAs sacrificial layer lattice-matched to GaAs.[206–215]

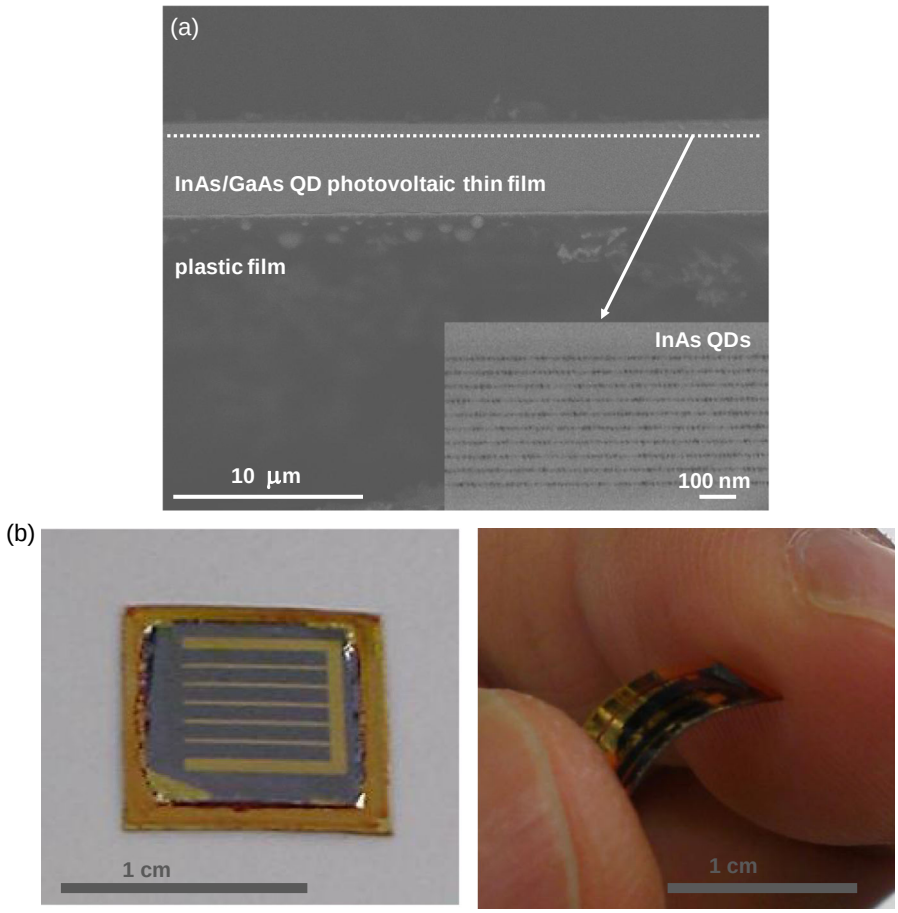

Figure 9. Flexible thin-film InAs/GaAs quantum dot (QD) solar cell: a) cross-sectional scanning electron microscope image and b) bird's eye view photographs. Inset of (a) is a cross-sectional tunneling electron microscope image of the InAs QD layers. Reproduced with permission.[200] Copyright 2012, American Institute of Physics.

Similarly, epitaxial liftoff of InP has also been studied, which utilizes selective etching of $In_{0.5}Ga_{0.5}As$ lattice-matched to InP.[216,217] By using these epitaxial liftoff techniques, multiple-time reuse of the original GaAs and InP wafers as growth seeds for thin-film solar cells was demonstrated.[210,213,216] Other than the scheme of selective wet chemical etching of a lattice-matched sacrificial layer, some mechanical liftoff techniques have been proposed and demonstrated.[218–224] Also for crystalline Si solar cells, producing multiple thin-film cells from a single Si wafer would be a cost-effective approach, which is comprehensively reviewed by the literature.[225,226] Slicing Si wafers can be achieved through mechanical delamination,[219,220,222,223] cleavage at porous-Si layers formed by anodic oxidation,[227–229] and ion-implantation-induced exfoliation.[230] Ion-implantation-induced exfoliation can also be applied to other semiconductor materials such as Ge and InP wafers. Alternative growth substrates of Ge[231] and InP[232] thin films were prepared by layer transfer using wafer-bonding and implantation-induced exfoliation onto Si substrates, which are significantly less expensive. InGaP/GaAs dual-junction and InGaAs single-junction solar cells were then grown on these Ge/Si and InP/Si alternative substrates, exhibiting comparable efficiencies relative to the reference cells grown on bulk Ge and InP substrates, respectively.

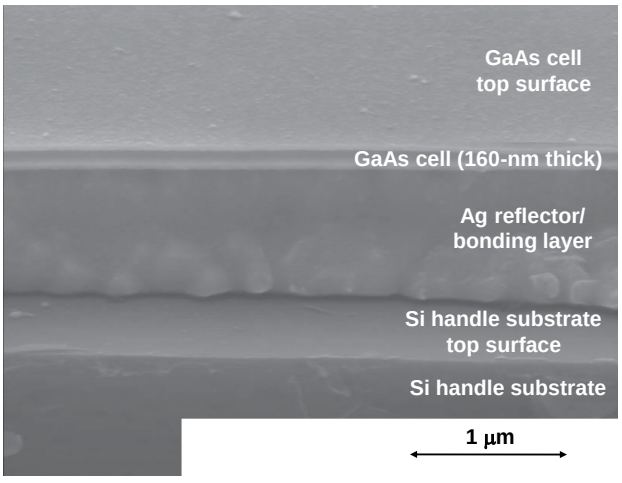

Figure 10. Bird's eye view scanning microscope image of the ultrathin GaAs solar cell on a metal mirror structure, fabricated by wafer bonding and layer transfer.[202]

6. Conclusions

This article reviewed various semiconductor wafer-bonding techniques for producing high-performance solar cells, as well as the types of cells fabricated using these techniques. Conventionally, multijunction solar cell designs focused on either lattice-matched or metamorphic growth approaches, which inevitably result in less design flexibility or lower material quality than desired. A promising alternative is the use of directly bonded interconnects between subcells, which allows for dislocation-free active regions by confining the defect network needed for lattice mismatch accommodation to tunnel junction interfaces. This approach enables monolithic interconnection without threading dislocations or planar defects, which commonly occur during lattice-mismatched epitaxial heterostructure growth. Semiconductor wafer bonding thus offers the capability to fabricate multijunction solar cells with ideal semiconductor bandgap combinations, free from the lattice-match restriction. Moreover, it provides design flexibility for solar cell structures, allowing for the integration of photovoltaic layers of arbitrary thickness onto any substrate. These technical advantages make wafer bonding a promising method for lower-cost production of solar cells and modules, such as by enabling the reuse of crystalline semiconductor wafers. Overall, semiconductor wafer-bonding technologies have the potential to pave the way for high-efficiency, low-cost solar energy conversion.

Conflict of Interest

The author declare no conflict of interest.

Keywords

devices, heterostructures, interfaces, multijunctions, optoelectronics, photovoltaics, surfaces

Received: April 28, 2023
Revised: August 15, 2023
Published online: August 31, 2023

[1] R. C. Willson, H. S. Hudson, *Nature* **1991**, *351*, 42.
[2] G. Kopp, J. L. Lean, *Geophys. Res. Lett.* **2011**, *38*, L01706.
[3] J. M. Olson, S. R. Kurtz, A. E. Kibbler, P. A. Faine, *Appl. Phys. Lett.* **1990**, *56*, 623.
[4] K. A. Bertness, S. R. Kurtz, D. J. Friedman, A. E. Kibbler, C. Kramer, J. M. Olson, *Appl. Phys. Lett.* **1994**, *65*, 989.
[5] T. Takamoto, E. Ikeda, H. Kurita, *Appl. Phys. Lett.* **1997**, *70*, 381.
[6] F. Dimroth, U. Schubert, A. W. Bett, *IEEE Electron Device Lett.* **2000**, *21*, 209.
[7] R. R. King, D. C. Law, K. M. Edmondson, C. M. Fetzer, G. S. Kinsey, H. Yoon, R. A. Sherif, N. H. Karam, *Appl. Phys. Lett.* **2007**, *90*, 183516.
[8] W. Guter, J. Schone, S. P. Philipps, M. Steiner, G. Siefer, A. Wekkeli, E. Welser, E. Oliva, A. W. Bett, F. Dimroth, *Appl. Phys. Lett.* **2009**, *94*, 223504.
[9] I. García, I. Rey-Stolle, B. Galiana, C. A. Algora, *Appl. Phys. Lett.* **2009**, *94*, 053509.
[10] S. Guha, J. Yang, B. Yan, *Sol. Energy Mater. Sol. Cells* **2013**, *119*, 1.
[11] M. Boccard, M. Despeisse, J. Escarre, X. Niquille, G. Bugnon, S. Hänni, M. Bonnet-Eymar, F. Meillaud, C. Ballif, *IEEE J. Photovoltaics* **2014**, *4*, 1368.
[12] T. Matsui, K. Maejima, A. Bidiville, H. Sai, T. Koida, T. Suezaki, M. Matsumoto, K. Saito, I. Yoshida, M. Kondo, *Jpn. J. Appl. Phys.* **2015**, *54*, 08KB10.
[13] D.-J. You, S.-H. Kim, H. Lee, J.-W. Chung, S.-T. Hwang, Y.-H. Heo, S. Lee, H.-M. Lee, *Prog. Photovoltaics* **2015**, *23*, 973.
[14] H. Sai, T. Matsui, K. Matsubara, *Appl. Phys. Lett.* **2016**, *109*, 183506.
[15] T. J. Grassman, D. J. Chmielewski, S. D. Carnevale, J. A. Carlin, S. A. Ringel, *IEEE J. Photovoltaics* **2016**, *6*, 326.
[16] M. Feifel, D. Lackner, J. Schön, J. Ohlmann, J. Benick, G. Siefer, F. Predan, M. Hermle, F. Dimroth, *Sol. RRL* **2021**, *5*, 2000763.
[17] J. Y. Kim, K. Lee, N. E. Coates, D. Moses, T.-Q. Nguyen, M. Dante, A. J. Heeger, *Science* **2007**, *317*, 222.
[18] L. Dou, J. You, J. Yang, C.-C. Chen, Y. He, S. Murase, T. Moriarty, K. Emery, G. Li, Y. Yang, *Nat. Photonics* **2012**, *6*, 180.
[19] Y. Zhang, B. Kan, Y. Sun, Y. Wang, R. Xia, X. Ke, Y. Yi, C. Li, H. Yip, X. Wan, Y. Cao, Y. Chen, *Adv. Mater.* **2018**, *30*, 1707508.
[20] Z. Zheng, J. Wang, P. Bi, J. Ren, Y. Wang, Y. Yang, X. Liu, S. Zhang, J. Hou, *Joule* **2022**, *6*, 171.
[21] R. Lin, J. Xu, M. Wei, Y. Wang, Z. Qin, Z. Liu, J. Wu, K. Xiao, B. Chen, S. M. Park, G. Chen, H. R. Atapattu, K. R. Graham, J. Xu, J. Zhu, L. Li, C. Zhang, E. H. Sargent, H. Tan, *Nature* **2022**, *603*, 73.
[22] K. Xiao, Y.-H. Lin, M. Zhang, R. D. J. Oliver, X. Wang, Z. Liu, X. Luo, J. Li, D. Lai, H. Luo, R. Lin, J. Xu, Y. Hou, H. J. Snaith, H. Tan, *Science* **2022**, *376*, 762.
[23] J. P. Mailoa, C. D. Bailie, E. C. Johlin, E. T. Hoke, A. J. Akey, W. H. Nguyen, M. D. McGehee, T. Buonassisi, *Appl. Phys. Lett.* **2015**, *106*, 121105.
[24] A. Al-Ashouri, E. Köhnen, B. Li, A. Magomedov, H. Hempel, P. Caprioglio, J. A. Márquez, A. B. M. Vilches, E. Kasparavicius, J. A. Smith, N. Phung, D. Menzel, M. Grischek, L. Kegelmann, D. Skroblin, C. Gollwitzer, T. Malinauskas, M. Jošt, G. Matic, B. Rech, R. Schlatmann, M. Topic, L. Korte, A. Abate, B. Stannowski, D. Neher, M. Stolterfoht, T. Unold, V. Getautis, S. Albrecht, *Science* **2020**, *370*, 1300.
[25] K. Sveinbjörnsson, B. Li, S. Mariotti, E. Jarzembowski, L. Kegelmann, A. Wirtz, F. Frühauf, A. Weihrauch, R. Niemann, L. Korte, F. Fertig, J. W. Müller, S. Albrecht, *ACS Energy Lett.* **2022**, *7*, 2654.
[26] X. Luo, H. Luo, H. Li, R. Xia, X. Zheng, Z. Huang, Z. Liu, H. Gao, X. Zhang, S. Li, Z. Feng, Y. Chen, H. Tan, *Adv. Mater.* **2023**, *35*, 2207883.
[27] W. Stolz, Y. Horikoshi, M. Naganuma, *Jpn. J. Appl. Phys.* **1988**, *27*, L1140.
[28] H. Kroemer, T.-Y. Liu, P. M. Petroff, *J. Cryst. Growth* **1989**, *95*, 96.
[29] M. Sugo, Y. Takanashi, M. M. Aljassim, M. Yamaguchi, *J. Appl. Phys.* **1990**, *68*, 540.
[30] K. Samonji, H. Yonezu, Y. Takagi, K. Iwaki, N. Ohshima, J. K. Shin, K. Pak, *Appl. Phys. Lett.* **1996**, *69*, 100.
[31] J. G. Belk, J. L. Sudijono, X. M. Zhang, J. H. Neave, T. S. Jones, B. A. Joyce, *Phys. Rev. Lett.* **1997**, *78*, 475.
[32] T. Detchprohm, M. Yano, S. Sano, R. Nakamura, S. Mochiduki, T. Nakamura, H. Amano, I. Akasaki, *Jpn. J. Appl. Phys.* **2001**, *40*, L16.
[33] G. Springholz, K. Wiesauer, *Phys. Rev. Lett.* **2002**, *88*, 015507.
[34] J. Z. Li, J. Bai, J.-S. Park, B. Adekore, K. Fox, M. Carroll, A. Lochtefeld, Z. Shellenbarger, *Appl. Phys. Lett.* **2007**, *91*, 021114.
[35] A. E. Romanov, E. C. Young, F. Wu, A. Tyagi, C. S. Gallinat, S. Nakamura, S. P. DenBaars, J. S. Speck, *J. Appl. Phys.* **2011**, *109*, 103522.
[36] P. G. Callahan, B. B. Haidet, D. Jung, G. G. E. Seward, K. Mukherjee, *Phys. Rev. Mater.* **2018**, *2*, 081601.
[37] S. J. Addamane, D. M. Shima, A. Mansoori, G. Balakrishnan, *J. Appl. Phys.* **2020**, *128*, 225301.

[38] T. D. Riney, *J. Appl. Phys.* **1961**, *32*, 454.
[39] T. Nakamura, U.S. Patent *3,239,908*, **1966**.
[40] G. Wallis, D. I. Pomerantz, *J. Appl. Phys.* **1969**, *40*, 3946.
[41] F. Stern, J. M. Woodall, *J. Appl. Phys.* **1974**, *45*, 3904.
[42] J. B. Lasky, *Appl. Phys. Lett.* **1986**, *48*, 78.
[43] M. Shimbo, K. Furukawa, K. Fukuda, K. Tanzawa, *J. Appl. Phys.* **1986**, *60*, 2987.
[44] L. J. Huang, J. O. Chu, D. F. Canaperi, C. P. D'Emic, R. M. Anderson, S. J. Koester, H.-S. Philip Wong, *Appl. Phys. Lett.* **2001**, *78*, 1267.
[45] P. R. Morrow, C.-M. Park, S. Ramanathan, M. J. Kobrinsky, M. Harmes, *IEEE Electron Device Lett.* **2006**, *27*, 335.
[46] C. Convertino, C. B. Zota, H. Schmid, D. Caimi, L. Czornomaz, A. M. Ionescu, K. E. Moselund, *Nat. Electron.* **2021**, *4*, 162.
[47] W. S. Wong, T. Sands, N. W. Cheung, M. Kneissl, D. P. Bour, P. Mei, L. T. Romano, N. M. Johnson, *Appl. Phys. Lett.* **2000**, *77*, 2822.
[48] S. Lee, K. H. Kim, J. Ju, T. Jeong, C. Lee, J. H. Baek, *Appl. Phys. Express* **2011**, *4*, 066501.
[49] J. Chun, K. J. Lee, Y.-C. Leem, W.-M. Kang, T. Jeong, J. H. Baek, H. J. Lee, B.-J. Kim, S.-J. Park, *ACS Appl. Mater. Interfaces* **2014**, *6*, 19482.
[50] C. M. Kang, J. Y. Lee, D. J. Kong, J. P. Shim, S. Kim, S. H. Mun, S. Y. Choi, M. D. Park, J. Kim, D. S. Lee, *ACS Photonics* **2018**, *5*, 4413.
[51] K. Nishigaya, K. Tanabe, *ECS J. Solid State Sci. Technol.* **2020**, *9*, 086002.
[52] H. Park, A. W. Fang, S. Kodama, J. E. Bowers, *Opt. Express* **2005**, *13*, 9460.
[53] A. W. Fang, H. Park, O. Cohen, R. Jones, M. J. Paniccia, J. E. Bowers, *Opt. Express* **2006**, *14*, 9203.
[54] J. Van Campenhout, P. Rojo-Romeo, P. Regreny, C. Seassal, D. Van Thourhout, S. Verstuyft, L. Di Cioccio, J. M. Fedeli, C. Lagahe, R. Baets, *Opt. Express* **2007**, *15*, 6744.
[55] K. Tanabe, M. Nomura, D. Guimard, S. Iwamoto, Y. Arakawa, *Opt. Express* **2009**, *17*, 7036.
[56] S. Palit, J. Kirch, G. Tsvid, L. Mawst, T. Kuech, N. M. Jokerst, *Opt. Lett.* **2009**, *34*, 2802.
[57] K. Tanabe, D. Guimard, D. Bordel, S. Iwamoto, Y. Arakawa, *Opt. Express* **2010**, *18*, 10604.
[58] D. Liang, X. Huang, G. Kurczveil, M. Fiorentino, R. G. Beausoleil, *Nat. Photonics* **2016**, *10*, 719.
[59] G. Crosnier, D. Sanchez, S. Bouchoule, P. Monnier, G. I. Sagnes, R. Raj, F. Raineri, *Nat. Photonics* **2017**, *11*, 297.
[60] Y. Kuo, H.-W. Chen, J. E. Bowers, *Opt. Express* **2008**, *16*, 9936.
[61] R. Takigawa, E. Higurashi, T. Suga, T. Kawanishi, *Opt. Express* **2011**, *19*, 15739.
[62] J.-H. Han, F. Boeuf, J. Fujikata, S. Takahashi, S. Takagi, M. Takenaka, *Nat. Photonics* **2017**, *11*, 486.
[63] H. Park, A. W. Fang, R. Jones, O. Cohen, O. Raday, M. N. Sysak, M. J. Paniccia, J. E. Bowers, *Opt. Express* **2007**, *15*, 6044.
[64] L. Chen, P. Dong, M. Lipson, *Opt. Express* **2008**, *16*, 11513.
[65] S.-H. Kim, D.-M. Geum, M.-S. Park, H.-S. Kim, J. D. Song, W. J. Choi, *Appl. Phys. Lett.* **2017**, *110*, 153505.
[66] H. Yamaguchi, S. Fujino, T. Hattori, Y. Hamakawa, *Jpn. J. Appl. Phys.* **1995**, *34*, L199.
[67] F. E. Ejeckam, Y. H. Lo, S. Subramanian, H. Q. Hou, B. E. Hammons, *Appl. Phys. Lett.* **1997**, *70*, 1685.
[68] S. Noda, K. Tomoda, N. Yamamoto, A. Chutinan, *Science* **2000**, *289*, 604.
[69] H. Ko, K. Takei, R. Kapadia, S. Chuang, H. Fang, P. W. Leu, K. Ganapathi, E. Plis, H. S. Kim, S.-Y. Chen, M. Madsen, A. C. Ford, Y.-L. Chueh, S. Krishna, S. Salahuddin, A. Javey, *Nature* **2010**, *468*, 286.
[70] R.-H. Kim, D.-H. Kim, J. Xiao, B. H. Kim, S.-I. Park, B. Panilaitis, R. Ghaffari, J. Yao, M. Li, Z. Liu, V. Malyarchuk, D. G. Kim, A.-P. Le, R. G. Nuzzo, D. L. Kaplan, F. G. Omenetto, Y. Huang, Z. Kang, J. A. Rogers, *Nat. Mater.* **2010**, *9*, 929.
[71] M. Madsen, K. Takei, R. Kapadia, H. Fang, H. Ko, T. Takahashi, A. C. Ford, M. H. Lee, A. Javey, *Adv. Mater.* **2011**, *23*, 3115.
[72] K. Hara, S. Matsumoto, T. Onda, W. Nagashima, I. Shoji, *Appl. Phys. Express* **2012**, *5*, 052201.
[73] W. Wei, Y. Zhang, Q. Xu, H. Wei, Y. Fang, Q. Wang, Y. Deng, T. Li, A. Gruverman, L. Cao, J. Huang, *Nat. Photonics* **2017**, *11*, 315.
[74] M. A. Tran, C. Zhang, T. J. Morin, L. Chang, S. Barik, Z. Yuan, W. Lee, G. Kim, A. Malik, Z. Zhang, J. Guo, H. Wang, B. Shen, L. Wu, K. Vahala, J. E. Bowers, H. Park, T. Komljenovic, *Nature* **2022**, *610*, 54.
[75] Q.-Y. Tong, U. Gösele, *Semiconductor Wafer Bonding: Science and Technology*, Wiley, NJ **1998**.
[76] *Silicon Wafer Bonding Technology for VLSI and MEMS Applications* (Eds: S. S. Iyer, A. J. Auberton-Herve), IEE, London **2002**.
[77] *Wafer Bonding: Applications and Technology* (Eds: M. Alexe, U. Gösele), Springer, Berlin **2004**.
[78] *Handbook of Wafer Bonding* (Eds: P. Ramm, J. J. Lu, M. M. V. Taklo), Wiley, Weinheim **2012**.
[79] J. Haisma, B. A. C. M. Spierings, U. K. P. Biermann, A. A. van Gorkum, *Appl. Opt.* **1994**, *33*, 1154.
[80] A. Black, A. R. Hawkins, N. M. Margalit, D. I. Babic, A. L. Holmes, Y.-L. Chang, P. Abraham, J. E. Bowers, E. L. Hu, *IEEE J. Sel. Top. Quantum Electron.* **1997**, *3*, 943.
[81] Q.-Y. Tong, U. M. Goesele, *Adv. Mater.* **1999**, *11*, 1409.
[82] G. K. Celler, S. Cristoloveanu, *J. Appl. Phys.* **2003**, *93*, 4955.
[83] G. Taraschi, A. J. Pitera, E. A. Fitzgerald, *Solid-State Electron.* **2004**, *48*, 1297.
[84] O. Moutanabbir, U. Gösele, *Ann. Rev. Mater. Res.* **2010**, *40*, 469.
[85] L. D. Cioccio, P. Gueguen, R. Taibi, D. Landru, G. Gaudin, C. Chappaz, F. Rieutord, F. de Crecy, I. Radu, L. L. Chapelon, L. Clavelier, *J. Electrochem. Soc.* **2011**, *158*, P81P86.
[86] T. Mizumoto, Y. Shoji, R. Takei, *Materials* **2012**, *5*, 9851004.
[87] L. Granados, R. Morena, N. Takamure, T. Suga, S. J. Huang, D. R. McKenzie, A. Ho-Baillie, *Mater. Today* **2021**, *47*, 131.
[88] N. Shigekawa, J. Liang, Y. Ohno, *Jpn. J. Appl. Phys.* **2022**, *61*, 120101.
[89] U. Goesele, H. Stenzel, T. Martini, J. Steinkirchner, D. Conrad, K. Scheerschmidt, *Appl. Phys. Lett.* **1995**, *67*, 3614.
[90] G. Kastner, O. Breitenstein, R. Scholz, M. Reiche, *J. Mater. Sci.* **2002**, *13*, 593.
[91] N. Daix, E. Uccelli, L. Czornomaz, D. Caimi, C. Rossel, M. Sousa, H. Siegwart, C. Marchiori, J. M. Hartmann, K.-T. Shiu, C.-W. Cheng, M. Krishnan, M. Lofaro, M. Kobayashi, D. Sadana, J. Fompeyrine, *APL Mater.* **2014**, *2*, 086104.
[92] M. Tedjini, F. Fournel, H. Moriceau, V. Larrey, D. Landru, O. Kononchuk, S. Tardif, F. Rieutord, *Appl. Phys. Lett.* **2016**, *109*, 111603.
[93] K. Tanabe, *Jpn. J. Appl. Phys.* **2021**, *60*, 055504.
[94] I. Kudman, R. J. Paff, *J. Appl. Phys.* **1972**, *43*, 3760.
[95] S. Adachi, *J. Appl. Phys.* **1982**, *53*, 8775.
[96] V. K. Yang, M. Groenert, C. W. Leitz, A. J. Pitera, M. T. Currie, E. A. Fitzgerald, *J. Appl. Phys.* **2003**, *93*, 3859.
[97] K. Tanabe, A. Fontcuberta i Morral, H. A. Atwater, D. J. Aiken, M. W. Wanlass, *Appl. Phys. Lett.* **2006**, *89*, 102106.
[98] F. Dimroth, M. Grave, P. Beutel, U. Fiedeler, C. Karcher, T. N. D. Tibbits, E. Oliva, G. Siefer, M. Schachtner, A. Wekkeli, A. W. Bett, R. Krause, M. Piccin, N. Blanc, C. Drazek, E. Guiot, B. Ghyselen, T. Salvetat, A. Tauzin, T. Signamarcheix, A. Dobrich, T. Hannappel, K. Schwarzburg, *Prog. Photovoltaics* **2014**, *22*, 227.
[99] F. Dimroth, T. N. D. Tibbits, M. Niemeyer, F. Predan, P. Beutel, C. Karcher, E. Oliva, G. Siefer, D. Lackner, P. Fuß-Kailuweit, A. W. Bett, R. Krause, C. Drazek, E. Guiot, J. Wasselin, A. Tauzin, T. Signamarcheix, *IEEE J. Photovoltaics* **2016**, *6*, 343.

[100] M. A. Green, E. D. Dunlop, G. Siefer, M. Yoshita, N. Kopidakis, K. Bothe, X. Hao, *Prog. Photovoltaics* **2023**, *31*, 3.
[101] P. T. Chiu, D. C. Law, R. L. Woo, S. B. Singer, D. Bhusari, W. D. Hong, A. Zakaria, J. Boisvert, S. Mesropian, R. R. King, N. H. Karam, *IEEE J. Photovoltaics* **2014**, *4*, 493.
[102] X. Sheng, C. A. Bower, S. Bonafede, J. W. Wilson, B. Fisher, M. Meitl, H. Yuen, S. Wang, L. Shen, A. R. Banks, C. J. Corcoran, R. G. Nuzzo, S. Burroughs, J. A. Rogers, *Nat. Mater.* **2014**, *13*, 593.
[103] P. Dai, S. Lu, S. Uchida, L. Ji, Y. Wu, M. Tan, L. Bian, H. Yang, *Appl. Phys. Express* **2016**, *9*, 016501.
[104] M. Wanlass, P. Ahrenkiel, D. Albin, J. Carapella, A. Duda, K. Emery, D. Friedman, J. Geisz, K. Jones, A. Kibbler, J. Kiehl, S. Kurtz, W. McMahon, T. Moriarty, J. Olson, A. Ptak, M. Romero, S. Ward, in *Proc. 4th World Conf. Photovoltaic Energy Conversion*, IEEE, Piscataway, NJ **2006**, pp. 729–732, https://doi.org/10.1109/WCPEC.2006.279559.
[105] J. F. Geisz, S. Kurtz, M. W. Wanlass, J. S. Ward, A. Duda, D. J. Friedman, J. M. Olson, W. E. McMahon, T. E. Moriarty, J. T. Kiehl, *Appl. Phys. Lett.* **2007**, *91*, 023502.
[106] J. F. Geisz, D. J. Friedman, J. S. Ward, A. Duda, W. J. Olavarria, T. E. Moriarty, J. T. Kiehl, M. J. Romero, A. G. Norman, K. M. Jones, *Appl. Phys. Lett.* **2008**, *93*, 123505.
[107] J. F. Geisz, M. A. Steiner, K. L. Schulte, M. Young, R. M. France, D. J. Friedman, *AIP Conf. Proc.* **2018**, *2012*, 040004.
[108] J. F. Geisz, R. M. France, K. L. Schulte, M. A. Steiner, A. G. Norman, H. L. Guthrey, M. R. Young, T. Song, T. Moriarty, *Nat. Energy* **2020**, *5*, 326.
[109] W. Shockley, H. J. Queisser, *J. Appl. Phys.* **1961**, *32*, 510.
[110] C. H. Henry, *J. Appl. Phys.* **1980**, *51*, 4494.
[111] N. Jain, K. L. Schulte, J. F. Geisz, D. J. Friedman, R. M. France, E. E. Perl, A. G. Norman, H. L. Guthrey, M. A. Steiner, *Appl. Phys. Lett.* **2018**, *112*, 053905.
[112] K. Tanabe, M. Nishioka, D. Guimard, S. Iwamoto, Y. Arakawa, in *25th European Photovoltaic Solar Energy Conf./5th World Conf. Photovoltaic Energy Conversion*, Valencia, 1DV.3.100 **2010**.
[113] K. Tanabe, K. Watanabe, Y. Arakawa, *Sci. Rep.* **2012**, *2*, 349.
[114] J. Yang, D. Cheong, J. Rideout, S. Tavakoli, R. Kleiman, in *Proc. 37th IEEE Photovoltaic Specialists Conf.*, IEEE, Piscataway, NJ **2011**, pp. 001019–001024, https://doi.org/10.1109/PVSC.2011.6186125.
[115] K. Derendorf, S. Essig, E. Oliva, V. Klinger, T. Roesener, S. P. Philipps, J. Benick, M. Hermle, M. Schachtner, G. Siefer, W. Jäger, F. Dimroth, *IEEE J. Photovoltaics* **2013**, *3*, 1423.
[116] S. Essig, C. Allebé, T. Remo, J. F. Geisz, M. A. Steiner, K. Horowitz, L. Barraud, J. S. Ward, M. Schnabel, A. Descoeudres, D. L. Young, M. Woodhouse, M. Despeisse, C. Ballif, A. Tamboli, *Nat. Energy* **2017**, *2*, 17144.
[117] R. Cariou, J. Benick, F. Feldmann, O. Höhn, H. Hauser, P. Beutel, N. Razek, M. Wimplinger, B. Bläsi, D. Lackner, M. Hermle, G. Siefer, S. W. Glunz, A. W. Bett, F. Dimroth, *Nat. Energy* **2018**, *3*, 326.
[118] P. Schygulla, R. Müller, D. Lackner, O. Höhn, H. Hauser, B. Bläsi, F. Predan, J. Benick, M. Hermle, S. W. Glunz, F. Dimroth, *Prog. Photovoltaics* **2022**, *30*, 869.
[119] A. Yamamoto, M. Yamaguchi, C. Uemura, *Appl. Phys. Lett.* **1985**, *47*, 975.
[120] M. B. Spitzer, C. J. Keavney, S. M. Vernon, V. E. Haven, *Appl. Phys. Lett.* **1987**, *51*, 364.
[121] M. S. Leite, R. L. Woo, J. N. Munday, W. D. Hong, S. Mesropian, D. C. Law, H. A. Atwater, *Appl. Phys. Lett.* **2013**, *102*, 033901.
[122] M. Wanlass, U.S. Patent *9,590,131*, **2017**.
[123] M. Yamaguchi, K. Ando, *J. Appl. Phys.* **1988**, *63*, 5555.
[124] C. J. Keavney, R. J. Walters, P. J. Drevinsky, *J. Appl. Phys.* **1993**, *73*, 60.
[125] R. Inoue, K. Tanabe, *Appl. Phys. Lett.* **2019**, *114*, 191101.
[126] R. Inoue, K. Tanabe, in *Proc. 46th IEEE Photovoltaic Specialists Conf.*, IEEE, Piscataway, NJ **2019**, pp. 0998–1000, https://doi.org/10.1109/PVSC40753.2019.8981299.
[127] B. Wakefield, M. A. G. Halliwell, T. Kerr, D. A. Andrews, G. J. Davies, D. R. Wood, *Appl. Phys. Lett.* **1984**, *44*, 341.
[128] M. S. Leite, R. L. Woo, W. D. Hong, D. C. Law, H. A. Atwater, *Appl. Phys. Lett.* **2011**, *98*, 093502.
[129] R. L. Woo, W. D. Hong, S. Mesropian, M. S. Leite, H. A. Atwater, D. C. Law, in *Proc. 37th IEEE Photovoltaic Specialists Conf.*, IEEE, Piscataway, NJ **2011**, pp. 000295–000298, https://doi.org/10.1109/PVSC.2011.6185903.
[130] C. W. Leitz, M. T. Currie, A. Y. Kim, J. Lai, E. Robbins, E. A. Fitzgerald, M. T. Bulsara, *J. Appl. Phys.* **2001**, *90*, 2730.
[131] M. R. Lueck, C. L. Andre, A. J. Pitera, M. L. Lee, E. A. Fitzgerald, S. A. Ringel, *IEEE Electron. Dev. Lett.* **2006**, *27*, 142.
[132] J. S. Ward, K. Ramanathan, F. S. Hasoon, T. J. Coutts, J. Keane, M. A. Contreras, T. Moriarty, R. A. Noufi, *Prog. Photovoltaics* **2002**, *10*, 41.
[133] R. Kamada, T. Yagioka, S. Adachi, A. Handa, K. F. Tai, T. Kato, H. Sugimoto, in *Proc. 43rd IEEE Photovoltaic Specialists Conf.*, IEEE, Piscataway, NJ **2016**, pp. 1287–1291, https://doi.org/10.1109/PVSC.2016.7749822.
[134] M. Nakamura, K. Yamaguchi, Y. Kimoto, Y. Yasaki, T. Kato, H. Sugimoto, *IEEE J. Photovoltaics* **2019**, *9*, 1863.
[135] A. Jasenek, U. Rau, K. Weinert, I. M. Kötschau, G. Hanna, G. Voorwinden, M. Powalla, H. W. Schock, J. H. Werner, *Thin Solid Films* **2001**, *387*, 228.
[136] S. Kawakita, M. Imaizumi, T. Sumita, K. Kushiya, T. Ohshima, M. Yamaguchi, S. Matsuda, S. Yoda, T. Kamiya, in *Proc. 3rd World Conf. Photovoltaic Energy Conversion*, IEEE, Piscataway, NJ **2003**, pp. 693–696.
[137] S. Kawakita, M. Imaizumi, K. Makita, J. Nishinaga, T. Sugaya, H. Shibata, S. Sato, T. Ohshima, in *Proc. 43rd IEEE Photovoltaic Specialists Conf.*, IEEE, Piscataway, NJ **2016**, pp. 2574–2577, https://doi.org/10.1109/PVSC.2016.7750113.
[138] K. Makita, Y. Kamikawa, T. Koida, H. Mizuno, R. Oshima, Y. Shoji, S. Ishizuka, T. Takamoto, T. Sugaya, *Prog. Photovoltaics* **2023**, *31*, 71.
[139] C. W. Tang, *Appl. Phys. Lett.* **1986**, *48*, 183.
[140] G. Yu, J. Gao, J. C. Hummelen, F. Wudl, A. J. Heeger, *Science* **1995**, *270*, 1789.
[141] B. A. Gregg, M. C. Hanna, *J. Appl. Phys.* **2003**, *93*, 3605.
[142] R. C. Chiechi, R. W. A. Havenith, J. C. Hummelen, L. J. A. Koster, M. A. Loi, *Mater. Today* **2013**, *16*, 281.
[143] M. Granström, K. Petritsch, A. C. Arias, A. Lux, M. R. Andersson, R. H. Friend, *Nature* **1998**, *395*, 257.
[144] L. Chen, P. Degenaar, D. D. C. Bradley, *Adv. Mater.* **2008**, *20*, 1679.
[145] K.-H. Yim, Z. Zheng, Z. Liang, R. H. Friend, W. T. S. Huck, J.-S. Kim, *Adv. Funct. Mater.* **2008**, *18*, 1012.
[146] A. Tada, Y. Geng, Q. Wei, K. Hashimoto, K. Tajima, *Nat. Mater.* **2011**, *10*, 450.
[147] L. M. Fraas, J. E. Avery, V. S. Sundaram, V. T. Kinh, T. M. Davenport, J. W. Yerkes, J. M. Gee, K. A. Emery, in *Proc. 21st IEEE Photovoltaic Specialists Conf.*, IEEE, Piscataway, NJ **1990**, pp. 190–195, https://doi.org/10.1109/PVSC.1990.111616.
[148] T. Takamoto, E. Ikeda, T. Agui, H. Kurita, T. Tanabe, S. Tanaka, H. Matsubara, Y. Mine, S. Takagishi, M. Yamaguchi, in *Proc. 26th IEEE Photovoltaic Specialists Conf.*, IEEE, Piscataway, NJ **1997**, pp. 1031–1034, https://doi.org/10.1109/PVSC.1997.654265.
[149] H. Matsubara, T. Tanabe, A. Moto, Y. Mine, S. Takagishi, *Sol. Energy Mater. Sol. Cells* **1998**, *50*, 177.
[150] T. Yamada, A. Moto, Y. Iguchi, M. Takahashi, S. Tanaka, T. Tanabe, S. Takagishi, *Jpn. J. Appl. Phys.* **2005**, *44*, L988.

[151] R. Inoue, N. Takehara, T. Naito, K. Tanabe, *ACS Appl. Electron. Mater.* **2019**, *1*, 936.
[152] H. C. Lin, K. L. Chang, K. C. Hsieh, K. Y. Cheng, W. H. Wang, *J. Appl. Phys.* **2002**, *92*, 4132.
[153] D. Andrijasevic, M. Austerer, A. M. Andrews, P. Klang, W. Schrenk, G. Strasser, *Appl. Phys. Lett.* **2008**, *92*, 051117.
[154] D. Kasahara, D. Morita, T. Kosugi, K. Nakagawa, J. Kawamata, Y. Higuchi, H. Matsumura, T. Mukai, *Appl. Phys. Express* **2011**, *4*, 072103.
[155] Y.-H. Jhang, K. Tanabe, S. Iwamoto, Y. Arakawa, *IEEE Photonics Technol. Lett.* **2015**, *27*, 875.
[156] Y.-C. Li, L.-B. Chang, M.-J. Jeng, T.-E. Nee, J.-H. Hsieh, C.-N. Chang, H.-Z. Luo, Y.-C. Li, *J. Electron. Mater.* **2020**, *49*, 6859.
[157] E. Ide, S. Angata, A. Hirose, K. F. Kobayashi, *Acta Mater.* **2005**, *53*, 2385.
[158] R. Takigawa, E. Higurashi, T. Suga, R. Sawada, *Appl. Phys. Express* **2008**, *1*, 112201.
[159] T. Morita, E. Ide, Y. Yasuda, A. Hirose, K. Kobayashi, *Jpn. J. Appl. Phys.* **2008**, *47*, 6615.
[160] Y. Morisada, T. Nagaoka, M. Fukusumi, Y. Kashiwagi, M. Yamamoto, M. Nakamoto, *J. Electron. Mater.* **2010**, *39*, 1283.
[161] H. Mizuno, K. Makita, K. Matsubara, *Appl. Phys. Lett.* **2012**, *101*, 191111.
[162] W. E. McMahon, C.-T. Lin, J. S. Ward, J. F. Geisz, M. W. Wanlass, J. J. Carapella, W. Olavarría, M. Young, M. A. Steiner, R. M. France, A. E. Kibbler, A. Duda, J. M. Olson, E. E. Perl, D. J. Friedman, J. E. Bowers, *IEEE J. Photovoltaics* **2013**, *3*, 868.
[163] J. Yang, Z. Peng, D. Cheong, R. Kleiman, *IEEE J. Photovoltaics* **2014**, *4*, 1149.
[164] C.-T. Lin, W. E. McMahon, J. S. Ward, J. F. Geisz, M. W. Wanlass, J. J. Carapella, W. Olavarria, E. E. Perl, M. Young, M. A. Steiner, R. M. France, A. E. Kibbler, A. Duda, T. E. Moriarty, D. J. Friedman, J. E. Bowers, *Prog. Photovoltaics* **2015**, *23*, 593.
[165] T. Hishida, J. Liang, N. Shigekawa, *Jpn. J. Appl. Phys.* **2020**, *59*, SBBB04.
[166] K. Makita, H. Mizuno, T. Tayagaki, T. Aihara, R. Oshima, Y. Shoji, H. Sai, H. Takato, R. Müller, P. Beutel, D. Lackner, J. Benick, M. Hermle, F. Dimroth, T. Sugaya, *Prog. Photovoltaics* **2020**, *28*, 16.
[167] T. Sameshima, J. Takenezawa, M. Hasumi, T. Koida, T. Kaneko, M. Karasawa, M. Kondo, *Jpn. J. Appl. Phys.* **2011**, *50*, 052301.
[168] S. Yoshidomi, J. Furukawa, M. Hasumi, T. Sameshima, *Energy Procedia* **2014**, *60*, 116.
[169] A. C. Tamboli, M. F. A. M. van Hest, M. A. Steiner, S. Essig, E. E. Perl, A. G. Norman, N. Bosco, P. Stradins, *Appl. Phys. Lett.* **2015**, *106*, 263904.
[170] N. Shigekawa, T. Hara, T. Ogawa, J. Liang, T. Kamioka, K. Araki, M. Yamaguchi, *IEEE J. Photovoltaics* **2018**, *8*, 879.
[171] T. Yamashita, S. Hirata, R. Inoue, K. Kishibe, K. Tanabe, *Adv. Mater. Interfaces* **2019**, *6*, 1900921.
[172] K. Kishibe, K. Tanabe, *Appl. Phys. Lett.* **2019**, *115*, 081601.
[173] T. R. Klein, B. G. Lee, M. Schnabel, E. L. Warren, P. Stradins, A. C. Tamboli, M. F. A. M. van Hest, *ACS Appl. Mater. Interfaces* **2018**, *10*, 8086.
[174] A. Boca, J. C. Boisvert, D. C. Law, S. Mesropian, N. H. Karam, W. D. Hong, R. L. Woo, D. M. Bhusari, E. Turevskaya, P. Mack, P. Glatkowski, in *Proc. 35th IEEE Photovoltaic Specialists Conf.*, IEEE, Piscataway, NJ **2010**, pp. 003310–003315, https://doi.org/10.1109/PVSC.2010.5617076.
[175] Q.-Y. Tong, R. Gafiteanu, U. Gösele, *J. Electrochem. Soc.* **1992**, *139*, L101.
[176] K. Kishibe, S. Hirata, R. Inoue, T. Yamashita, K. Tanabe, *Nanomaterials* **2019**, *9*, 1742.
[177] N. Sano, K. Nishigaya, K. Tanabe, *Appl. Phys. Lett.* **2022**, *121*, 011601.
[178] K. Okamoto, K. Kishibe, N. Sano, K. Tanabe, *Appl. Phys. Express* **2023**, *16*, 036502.
[179] J. P. Thomas, K. T. Leung, *Adv. Funct. Mater.* **2014**, *24*, 4978.
[180] S. Jäckle, M. Mattiza, M. Liebhaber, G. Brönstrup, M. Romme, K. Lips, S. Christiansen, *Sci. Rep.* **2015**, *5*, 13008.
[181] K. Okamoto, Y. Fujita, K. Nishigaya, K. Tanabe, *PNAS Nexus* **2023**, *2*, pgad067.
[182] T. Trupke, M. A. Green, P. Würfel, *J. Appl. Phys.* **2002**, *92*, 1668.
[183] T. Trupke, M. A. Green, P. Würfel, *J. Appl. Phys.* **2002**, *92*, 4117.
[184] V. I. Klimov, *Appl. Phys. Lett.* **2006**, *89*, 123118.
[185] M. C. Hanna, A. J. Nozik, *J. Appl. Phys.* **2006**, *100*, 074510.
[186] K. Tanabe, *Electron. Lett.* **2007**, *43*, 998.
[187] P. Gibart, F. Auzel, J. C. Guillaume, K. Zahraman, *Jpn. J. Appl. Phys.* **1996**, *35*, 4401.
[188] M. Wolf, R. Brendel, J. H. Werner, H. J. Queisser, *J. Appl. Phys.* **1998**, *83*, 4213.
[189] R. D. Schaller, V. I. Klimov, *Phys. Rev. Lett.* **2004**, *92*, 186601.
[190] R. J. Ellingson, M. C. Beard, J. C. Johnson, P. R. Yu, O. I. Micic, A. J. Nozik, A. Shabaev, A. L. Efros, *Nano Lett.* **2005**, *5*, 865.
[191] T. Fukuda, S. Kato, E. Kin, K. Okaniwa, H. Morikawa, Z. Honda, N. Kamata, *Opt. Mater.* **2009**, *32*, 22.
[192] P. M. Stella, R. M. Kurland, H. G. Mesch, in *Proc. 23rd IEEE Photovoltaic Specialists Conf.*, IEEE, Piscataway, NJ **1993**, pp. 21–26, https://doi.org/10.1109/PVSC.1993.347084.
[193] A. Takano, T. Kamoshita, *Jpn. J. Appl. Phys.* **2004**, *43*, 7976.
[194] K. M. Edmondson, D. C. Law, G. Glenn, A. Paredes, R. R. King, N. H. Karam, in *Proc. 4th World Conf. Photovoltaic Energy Conversion*, IEEE, Piscataway, NJ **2006**, pp. 1935–1938, https://doi.org/10.1109/WCPEC.2006.279876.
[195] J. Yoon, A. J. Baca, S.-I. Park, P. Elvikis, J. B. Geddes, III, L. Li, R. H. Kim, J. Xiao, S. Wang, T.-H. Kim, M. J. Motala, B. Y. Ahn, E. B. Duoss, J. A. Lewis, R. G. Nuzzo, P. M. Ferreira, Y. Huang, A. Rockett, J. A. Rogers, *Nat. Mater.* **2008**, *7*, 907.
[196] K.-T. Shiu, J. Zimmerman, H. Wang, S. R. Forrest, *Appl. Phys. Lett.* **2009**, *95*, 223503.
[197] Z. Fan, H. Razavi, J. Do, A. Moriwaki, O. Ergen, Y.-L. Chueh, P. W. Leu, J. C. Ho, T. Takahashi, L. A. Reichertz, S. Neale, K. Yu, M. Wu, J. W. Ager, A. Javey, *Nat. Mater.* **2009**, *8*, 648.
[198] S. Ishizuka, T. Yoshiyama, K. Mizukoshi, A. Yamada, S. Niki, *Sol. Energy Mater. Sol. Cells* **2010**, *94*, 2052.
[199] R. J. Knuesel, H. O. Jacobs, *Proc. Natl. Acad. Sci. U.S.A.* **2010**, *107*, 993.
[200] K. Tanabe, K. Watanabe, Y. Arakawa, *Appl. Phys. Lett.* **2012**, *100*, 192102.
[201] M. Kaltenbrunner, M. S. White, E. D. Głowacki, T. Sekitani, T. Someya, N. S. Sariciftci, S. Bauer, *Nat. Commun.* **2012**, *3*, 770.
[202] K. Tanabe, K. Nakayama, H. A. Atwater, in *Proc. 33rd IEEE Photovoltaic Specialists Conf.*, IEEE, Piscataway, NJ **2008**, pp. 1–4, https://doi.org/10.1109/PVSC.2008.4922457.
[203] X. H. Li, P. C. Li, D. Z. Hu, D. M. Schaadt, E. T. Yu, *J. Appl. Phys.* **2013**, *114*, 044310.
[204] H.-L. Chen, A. Cattoni, R. De Lépinau, A. W. Walker, O. Höhn, D. Lackner, G. Siefer, M. Faustini, N. Vandamme, J. Goffard, B. Behaghel, C. Dupuis, N. Bardou, F. Dimroth, S. A. Collin, *Nat. Energy* **2019**, *4*, 761.
[205] B. M. Kayes, H. Nie, R. Twist, S. G. Spruytte, F. Reinhardt, I. C. Kizilyalli, G. S. Higashi, in *Proc. 37th IEEE Photovoltaic Specialists Conf.*, IEEE, Piscataway, NJ **2011**, pp. 000004–000008, https://doi.org/10.1109/PVSC.2011.6185831.
[206] G. A. Antypas, J. Edgecumbe, *Appl. Phys. Lett.* **1975**, *26*, 371.
[207] M. Konagai, M. Sugimoto, K. Takahashi, *J. Cryst. Growth* **1978**, *45*, 277.
[208] E. Yablonovitch, T. Gmitter, J. P. Harbison, R. Bhat, *Appl. Phys. Lett.* **1987**, *51*, 2222.

[209] A. van Geelen, P. R. Hageman, G. J. Bauhuis, P. C. van Rijsingen, P. Schmidt, L. J. Giling, *Mater. Sci. Eng. B* **1997**, *45*, 162.
[210] G. J. Bauhuis, P. Mulder, E. J. Haverkamp, J. J. Schermer, E. Bongers, G. Oomen, W. Köstler, G. Strobl, *Prog. Photovoltaics* **2010**, *18*, 155.
[211] J. Yoon, S. Jo, I. S. Chun, I. Jung, H.-S. Kim, M. Meitl, E. Menard, X. Li, J. J. Coleman, U. Paik, J. A. Rogers, *Nature* **2010**, *465*, 329.
[212] K. Lee, J. D. Zimmerman, X. Xiao, K. Sun, S. R. Forrest, *J. Appl. Phys.* **2012**, *111*, 033527.
[213] J. Adams, V. Elarde, A. Hains, C. Stender, F. Tuminello, C. Youtsey, A. Wibowo, M. Osowski, *IEEE J. Photovoltaics* **2013**, *3*, 899.
[214] C.-W. Cheng, K.-T. Shiu, N. Li, S.-J. Han, L. Shi, D. K. Sadana, *Nat. Commun.* **2013**, *4*, 1577.
[215] D.-M. Geum, M.-S. Park, J. Y. Lim, H.-D. Yang, J. D. Song, C. Z. Kim, E. Yoon, S.-H. Kim, W. J. Choi, *Sci. Rep.* **2016**, *6*, 20610.
[216] K. Lee, K.-T. Shiu, J. D. Zimmerman, C. K. Renshaw, S. R. Forrest, *Appl. Phys. Lett.* **2010**, *97*, 101107.
[217] F. Chancerel, P. Regreny, J. L. Leclercq, S. Brottet, M. Volatier, A. Jaouad, M. Darnon, S. Fafard, N. P. Blanchard, M. Gendry, V. Aimez, *Sol. Energy Mater. Sol. Cells* **2019**, *195*, 204.
[218] J. Park, P. A. Barnes, C. C. Tin, A. A. Allerman, *J. Cryst. Growth* **1998**, *187*, 185.
[219] A. J. Baca, M. A. Meitl, H. C. Ko, S. Mack, H.-S. Kim, J. Dong, P. M. Ferreira, J. A. Rogers, *Adv. Funct. Mater.* **2007**, *17*, 3051.
[220] C. H. Lee, D. R. Kim, I. S. Cho, N. William, Q. Wang, X. Zheng, *Sci. Rep.* **2012**, *2*, 1000.
[221] D. Shahrjerdi, S. W. Bedell1, C. Ebert, C. Bayram, B. Hekmatshoar, K. Fogel, P. Lauro, M. Gaynes, T. Gokmen, J. A. Ott, D. K. Sadana, *Appl. Phys. Lett.* **2012**, *100*, 053901.
[222] S. Saha, M. M. Hilali, E. U. Onyegam, D. Sarkar, D. Jawarani, R. A. Rao, L. Mathew, R. S. Smith, D. Xu, U. K. Das, B. Sopori, S. K. Banerjee, *Appl. Phys. Lett.* **2013**, *102*, 163904.
[223] P. Bellanger, A. Slaoui, A. Minj, R. Martini, M. Debucquoy, J. M. Serra, *IEEE J. Photovoltaics* **2016**, *6*, 1115.
[224] J. S. Mangum, A. D. Rice, J. Chen, J. Chenenko, E. W. K. Wong, A. K. Braun, S. Johnston, H. Guthrey, J. F. Geisz, A. J. Ptak, C. E. Packard, *Adv. Energy Mater.* **2022**, *12*, 2201332.
[225] R. Brendel, *Jpn. J. Appl. Phys.* **2001**, *40*, 4431.
[226] R. B. Bergmann, J. H. Werner, *Thin Solid Films* **2002**, *403–404*, 162.
[227] T. Yonehara, K. Sakaguchi, N. Sato, *Appl. Phys. Lett.* **1994**, *64*, 2108.
[228] C. S. Solanki, R. R. Bilyalov, J. Poortmans, J. Nijs, R. Mertens, *Sol. Energy Mater. Sol. Cells* **2004**, *83*, 101.
[229] A. Lukianov, K. Murakami, C. Takazawa, M. Ihara, *Appl. Phys. Lett.* **2016**, *108*, 213904.
[230] M. Bruel, *Electron. Lett.* **1995**, *31*, 1201.
[231] M. J. Archer, D. C. Law, S. Mesropian, M. Haddad, C. M. Fetzer, A. C. Ackerman, C. Ladous, R. R. King, H. A. Atwater, *Appl. Phys. Lett.* **2008**, *92*, 103503.
[232] J. M. Zahler, K. Tanabe, C. Ladous, T. Pinnington, F. D. Newman, H. A. Atwater, *Appl. Phys. Lett.* **2007**, *91*, 012108.

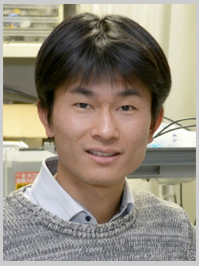

Katsuaki Tanabe received his B.Eng. (2001) and M.Eng. (2003) in chemical engineering from the University of Tokyo, and his M.S. (2005) in applied physics and Ph.D. (2008) in materials science from California Institute of Technology. He was a project assistant professor (2008–2011) and a project associate professor (2011–2015) at the Institute for Nano Quantum Information Electronics, University of Tokyo, and has been an associate professor in the Department of Chemical Engineering, Kyoto University, since 2015.